



HAL
open science

Structural elements made with highly flowable UHPFRC: Correlating computational fluid dynamics (CFD) predictions and non-destructive survey of fiber dispersion with failure modes

Liberato Ferrara, Massimiliano Cremonesi, Marco Faifer, Sergio Toscani, Luca Sorelli, Marc-Antoine Baril, Julien Réthoré, Florent Baby, François Toutlemonde, Sébastien Bernardi

► To cite this version:

Liberato Ferrara, Massimiliano Cremonesi, Marco Faifer, Sergio Toscani, Luca Sorelli, et al.. Structural elements made with highly flowable UHPFRC: Correlating computational fluid dynamics (CFD) predictions and non-destructive survey of fiber dispersion with failure modes. *Engineering Structures*, 2017, 133, pp.151-171. 10.1016/j.engstruct.2016.12.026 . hal-01499516

HAL Id: hal-01499516

<https://hal.science/hal-01499516>

Submitted on 10 May 2021

HAL is a multi-disciplinary open access archive for the deposit and dissemination of scientific research documents, whether they are published or not. The documents may come from teaching and research institutions in France or abroad, or from public or private research centers.

L'archive ouverte pluridisciplinaire **HAL**, est destinée au dépôt et à la diffusion de documents scientifiques de niveau recherche, publiés ou non, émanant des établissements d'enseignement et de recherche français ou étrangers, des laboratoires publics ou privés.



Distributed under a Creative Commons Attribution 4.0 International License

Structural elements made with highly flowable UHPFRC: Correlating computational fluid dynamics (CFD) predictions and non-destructive survey of fiber dispersion with failure modes

Liberato Ferrara ^{a,*}, Massimiliano Cremonesi ^a, Marco Faifer ^b, Sergio Toscani ^b, Luca Sorelli ^c, Marc-Antoine Baril ^c, Julien Réthoré ^d, Florent Baby ^e, François Toutlemonde ^e, Sébastien Bernardi ^f

^a Politecnico di Milano, Department of Civil and Environmental Engineering, Milano, Italy

^b Politecnico di Milano, Department of Electronical Engineering and Bioengineering, Milano, Italy

^c Université Laval, Department of Water and Civil Engineering, Quebec, Canada

^d Institut National de Sciences Appliquées de Lyon, Lyon, France

^e IFSTTAR, Université Paris-Est, Marne la Vallée, France

^f Lafarge-Holcim, Paris, France

Structural design with highly flowable Fibre Reinforced Concrete has to duly take into account the preferential alignment of fibers, which can be governed through the rheological properties of the fluid mixture and the casting process and by the geometry of the structure. The possibility of predicting the fiber alignment, by tailoring the casting process, and of non-destructively monitoring it, can foster more efficient structural applications and design approaches.

Focusing on UHPFRC slabs with pre-arranged casting defects, the flow-induced alignment of the fibers has been predicted by means of a suitable CFD modelling approach and hence monitored via a non-destructive method based on magnetic inductance properties of the fiber reinforced composite. The comparison between the assessed data on the fiber orientation and the crack patterns as visualized by image analysis supports the effectiveness of casting flow modelling and non-destructive fiber dispersion monitoring in supporting the structural design of elements made with highly flowable fiber reinforced cementitious composites.

1. Introduction

The advent of Ultra High Performance Fiber Reinforced Concrete and Cementitious Composites (UHPFRC, UHPFRCCs) on the construction market, a few decades ago, has paved the way for a novel approach to the concept and design of civil engineering structures and infrastructures.

On the one hand, the high deformation tolerance and energy dissipation capacity allows optimizing the dimensions of “conventional” structural elements (beam- and column-like) thanks to a more efficient structural use of the material. As a consequence, longer spans could be covered and higher load bearing capacity (or even larger lateral load resistance in the case of earthquake-resistant structures) could be achieved with reduced section dimensions, thus also reducing the self-supporting structural

burden [1–3]. The enhanced performances in the hardened state are often associated with a superior performance in the fresh state. From the architectural point of view hence structural functions and complex shapes, which are hard to be cast with conventional reinforced concrete, can be easily obtained with UHPFRC [4–7].

In this framework, the dispersion of fibers inside a structural element, which is well recognized as a crucial issue in the reliability of structures made of Fiber Reinforced Concrete and Cementitious Composites plays a twofold role [8,9].

First of all a non-uniform dispersion of fibers, with zones with a reduced amount of fibers, may seriously affect the load bearing capacity as well as trigger unexpected failure mechanisms. Previous researches have pointed out that the non-uniform dispersion of fibers most likely occurs due to the negative effects of high fiber contents on the rheological properties of the fresh mixture [10,11]. A successful casting of conventional Fibre Reinforced Concrete (FRC) usually requires compaction and/or vibration, which may cause sedimentation of fibers, whereas contributing to an uneven

* Corresponding author.

E-mail address: liberato.ferrara@polimi.it (L. Ferrara).

spatial distribution of material mechanical properties inside the element.

Secondly, thanks to the synergistic effect with the superior fresh-state performance of UHPFRC, the need for manual compaction and vibration is reduced, resulting into a randomly uniform dispersion of fibers as well as into a more uniform spatial distribution of the material properties in the hardened state [12]. It has been furthermore shown that, thanks to both a suitably balanced set of fresh state properties and to a careful design of the casting process, it is possible to effectively orientate the fibers along the direction of the casting flow [13–15]. Both controlling and monitoring the fiber orientation during the casting process, is the first fundamental step towards a promising “holistic” approach to tailor the structural performance of UHPFRC structural elements. That is, enforcing the orientation of fibers along the direction of the principal tensile stress within the structural element when in service, will allow a more efficient structural use of the material to be effectively pursued [16–40]. Preferential orientation of fibers also jeopardize the isotropic material behavior assumption; the resulting even strongly orthotropic mechanical behavior of the material has to be duly taken into account in structural design, most of all when dealing with slab and shell structures which experience complex biaxial stress field arising from different load combinations.

The aforementioned “holistic design approach” for structures made with highly flowable FRC relies on two main “pillars” [41,42]. First, a reliable tool is needed, which predicts the alignment of the fibers by considering the rheological material properties and the casting process, including the geometry and boundary conditions of the structure to be cast; then, the assessment of the fiber distribution through a non-destructive time- and cost-effective method becomes a crucial quality control procedure.

2. Non-destructive monitoring of fiber dispersion

The early works on non-destructive monitoring of fiber dispersion in FRC structural elements employed X-ray imaging [43]. Besides the safety concerns related to the use of X-ray equipment on industrial scale, it is worth remarking that such methods, which have been also widely used thereafter by several researchers, mainly as a pre-check of destructive analyses [11] are able to provide an immediate visualization of the discrete fiber reinforcement network inside the analyzed region of the element, mainly in the case of steel fibers. As a matter of fact, the thickness of the element, in order to have meaningful information from the images, has to be necessarily limited, as a function of the power of the employed equipment and of the X-ray absorption capacity of the material. Furthermore, the unavoidable “loss” of the third dimension may introduce some artifacts in the results of image processing, affecting any quantitative information, e.g. about local fiber density, which could be garnered from it. The higher the fiber dosage and the aspect ratio of the fiber, the more influence have these artifacts.

Electrical methods, based on the effects of the fibers on the resistivity/conductivity of the composite material, have received lots of attention up to very recent years [44,45]. Ozyurt et al. [46] employed the Alternate Current Impedance Spectroscopy (AC-IS) for the detection of fiber dispersion related issues and demonstrated its reliability as well as its sensitivity to fiber orientation, clumping, segregation, etc. by means of extensive comparison with results obtained from destructive methods. Attempts were also made to address the application of the aforementioned method to industrial scale problems [47]. The method consists of applying to the specimen a voltage excitation over a wide range of frequencies (e.g. 10 MHz–1 Hz) and measuring the amplitude and phase of the flowing current. When considering direct current

(DC) or low frequency alternate current (AC), the behavior is practically insulating. However, the impedance Z significantly drops under high frequency alternate current excitation as a result of the displacement current. When the real and imaginary parts of the calculated impedance are plotted on a Nyquist diagram, FCCs exhibit the so called dual-arc behavior, with two cusps, each of them represents a local minimum of the imaginary part of the impedance with respect to the real part. The rightmost cusp corresponds to the DC resistance across the electrodes, whose real part of the impedance R_m is essentially due to the matrix. Previous works have shown that it is weakly affected by the presence of the fibers. The leftmost, high frequency cusp is strictly related to the presence of conductive fibers in the matrix. It can be shown that the real part of the impedance R depends on the conductivity of the composite material. R_m and R can thus be used to estimate the concentration of the fibers by means of a simple mixture rule. In order to overcome the drawback of the sensitivity to moisture conditions, the so-called normalized resistivity is used:

$$\frac{R_m}{R} = 1 + [\sigma_{fibers}]V_f \quad (1)$$

where V_f is the fiber volume fraction and σ_{fibers} is the intrinsic conductivity of the fibers which, in the case of highly conductive fibers, only depends on their aspect ratio, which may affect the possibility to apply the method to the case of hybrid fiber reinforcement.

The method has been extensively employed to assess the influence of the fresh state performance on the dispersion and orientation of the fibers [12], clearly highlighting the better uniformity in fiber dispersion achievable through FR-SCC, together with a sensitivity to flow induced fiber alignment. Any direct quantitative comparison between, e.g., the concentration of fibers, as evaluated from Eq. (1) and data obtainable from destructive tests (e.g. crushing samples, separating and weighing fibers) could hardly be found in the literature. The need of a dedicated expensive instrumentation, required by the width of the employed frequency range, and the sensitivity of the method to the contact impedance between the surface electrodes and the structure surface, stand, so far, as the main hindrance to a wide application of the method at the industrial scale.

In order to overcome this problem, a method has been developed based on the evaluation of the equivalent capacitance between the electrodes of a probe which has to be simply laid on the surface of the structure under test. The technique allows assessing information about the average fiber concentration and their average direction. The measurement frequencies are relatively low (unto few hundreds of kilohertz) so that the required instrumentation is easily available and relatively inexpensive. However, the method suffers from high sensitivity to the humidity and to the coupling between the electrodes and the specimen.

Lataste et al. [48] employed a method based on low frequency resistance measurements, with a four electrode arrangement, aimed at reducing the effects of the poor electrical coupling. The method has been demonstrated to be effective in detecting orientation characteristics of the dispersed fiber reinforcement, because of the different resistance measured along the two directions at right angle to each other; a qualitative correlation with mechanical properties measured along the same directions as above was also provided [49,50]. The method is by the way not able to provide any quantitative information about the local average concentration of the fibers. This is mainly due to the strong sensitivity of the concrete matrix resistivity to aging, moisture content and presence of electrolytes in the pores, which also affect the measured resistivity, beside the effect of fiber concentration.

The effects of conductive fibers on the dielectric properties of the fiber reinforced composite have led to the development of another method, based on the measurement of the effective

permittivity through a coaxial probe and microwave reflectometry techniques [51]. Since the (known) fiber aspect ratio governs the capacitive behavior of the fibers and of the fiber reinforced composite, the local average concentration of fibers could be assessed by assuming a random fiber orientation. In view of this the method is not sensitive to a preferential alignment of the fibers.

Methods based on the study of heat transients and on the effect of fibers on the thermal diffusivity of the composite have been also tentatively applied for the non-destructive assessment of fiber concentration [52]. Temperature fields within a structural element can be easily surveyed through InfraRed (IR) thermography, but the slow propagation of temperature variations in thick members, which makes it difficult to provide a controlled input excitation over large areas, may limit the applicability of the method. More recently, a method based on micro-wave thermography has been developed and successfully applied to mortar specimens reinforced with different amounts of steel fibers [53].

X-ray Computed Tomography (CT) scans have been also widely employed in the last decade: as a matter of fact, they allow effective 3D visualization of the fiber network inside a FRC specimen [13,39,54–62], also in the case of non-conductive fibers [63], for which electrical methods cannot be applied. Limits on the

specimen size and the need of an image analysis software for the quantitative processing of the collected data are so far the main concern in promoting the method for wider use, especially at the industrial scale.

Similar techniques, but employing SEM backscattered electron imaging, have been recently applied for the determination of the spatial dispersion of polymeric microfibers in strain hardening cementitious composites [64].

Methods, which employ a probe sensitive to the magnetic properties of the steel fibers have been recently proposed and validated [65–69]. In particular, the method proposed by Faifer et al. [70], which has been employed in this work, relies on the fact that the steel fiber reinforced concrete is a mixture of two materials with very different magnetic permeability. The presence and the arrangement of the fibers modify the path of the magnetic field lines generated by the winding of a probe which results in a variation of its inductance. Fiber concentration can be quantitatively assessed by calibrating the method. Additionally the preferential orientation of the fibers can be estimated [71,19]. Besides its good sensitivity and robustness, the method also features an ease of use, due to a portable equipment, which just needs to be laid of the surface of a structural element, even sub-vertical ones, such as walls

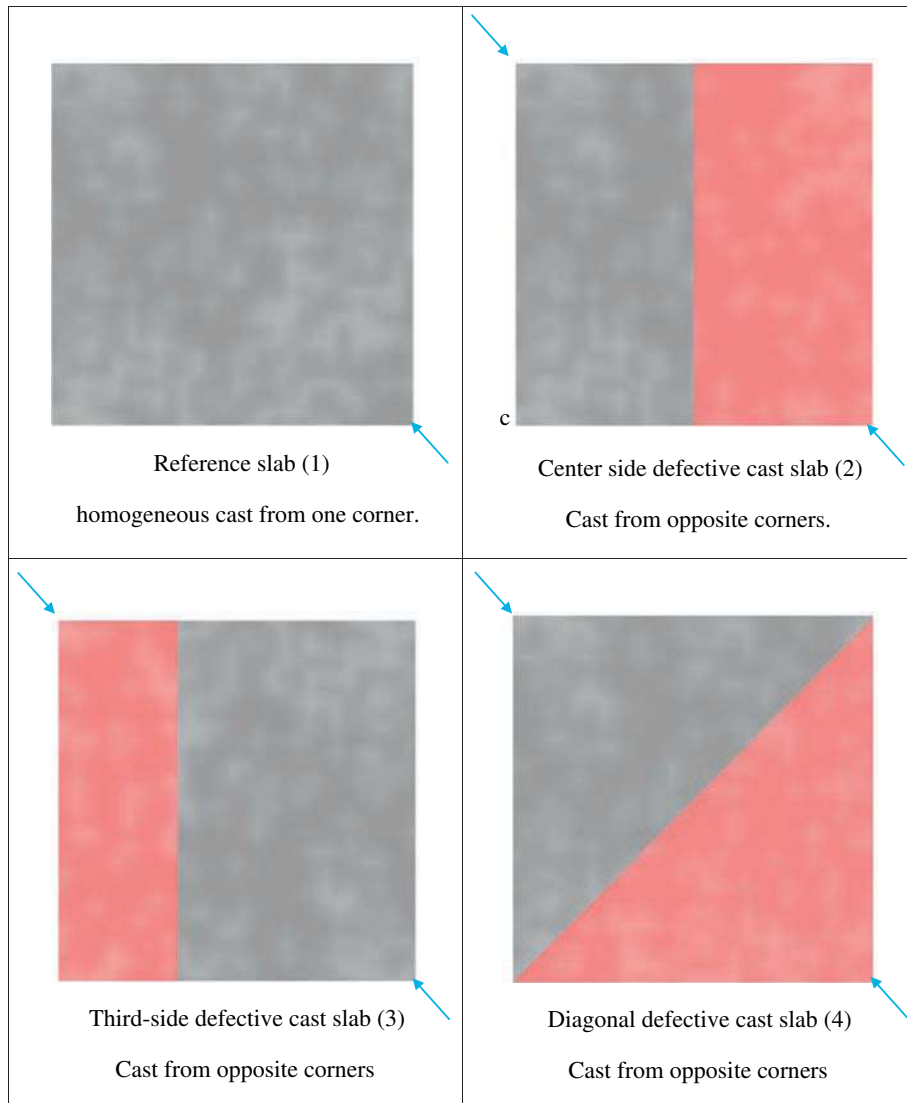


Fig. 1. Schematic of investigated slabs with position of pre-arranged defect – arrows indicate the pouring points and directions of the fresh HPRCC mixture.

or slabs accessible only from the bottom, without any dedicated care about the coupling between the element free surface and the sensor. The authors also tested a twin coil probe with the attempt of investigating also the dissipative effects due to the alternating magnetic field which invests the steel fibers [70].

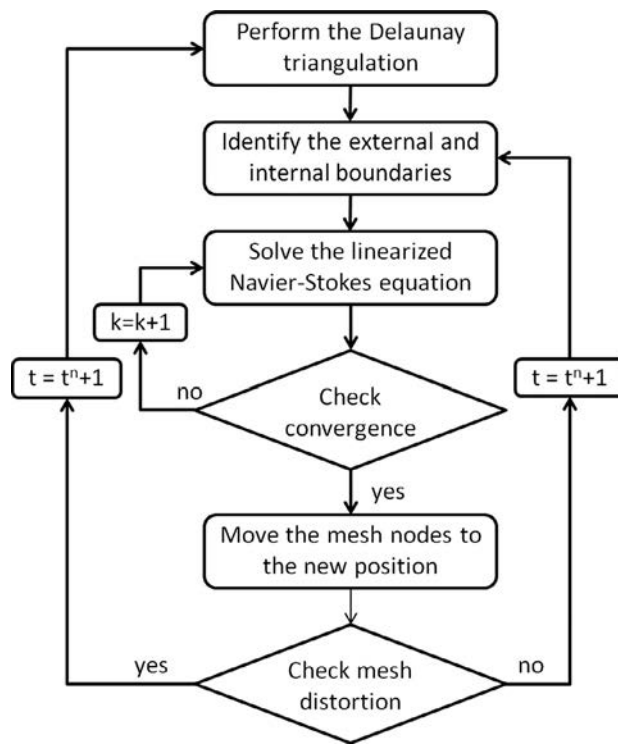
3. Numerical simulation of fresh concrete flow

The other “pillar” of the holistic design approach to structural applications made with highly flowable HPRCCs is represented by the predictive modelling approach for both the fresh state behavior of the material and the casting process as a whole. This research topic, contrary to investigation on non-destructive monitoring of fiber dispersion, which dates back to about 40 years ago, has started attracting interest of scientists and practitioners only in the very last decade, once again triggered by the tremendous

development in the field of Self Compacting/Highly Flowable Concrete and Cementitious Composites. Inspiration was drawn also from other fields of, e.g., industrial engineering, with reference to processes such as metal forming and die casting, which, by analogy, also casts a light over the application of this field of research in advanced casting techniques such as 3D printing and additive manufacturing [72].

To the present state, numerical modelling of fresh concrete flow is employed as a tool for both:

- (i) understanding the correlation between rheological properties of fresh concrete and mix proportions, and hence improve the entire mix-proportioning approach,
- (ii) as well as for the simulation of the casting process as a whole, including predictions of particle migration, flow blockages and, in case, fiber orientation.



Index of mesh distortion

for every element:

$$q_e = \sqrt{3}\alpha_e = \sqrt{3}\frac{R_e}{h_e} \gg 1$$

where R_e is the radius of a circumscribed circle and h_e is the element size.

The quality of the entire mesh is then evaluated by an arithmetic mean:

$$Q = \frac{1}{N_{el}} \sum_{e=1}^{N_{el}} q_e$$

The mesh is regenerated only if:

$$Q > \beta$$

Fig. 2. Flow chart of the employed numerical approach including re-meshing scheme based on mesh distortion.

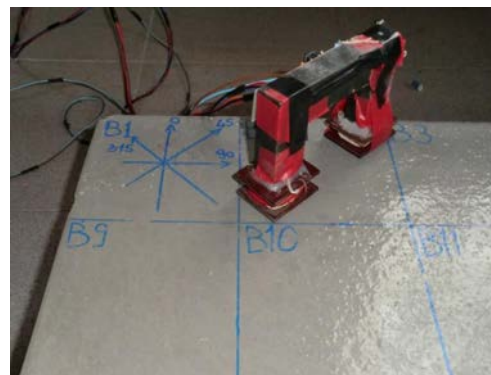
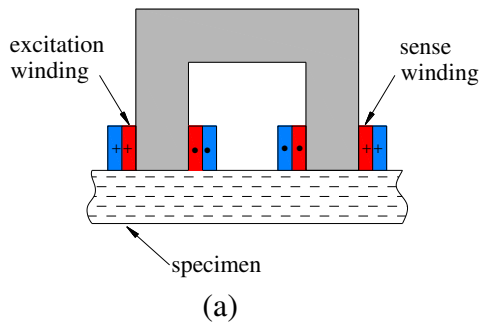


Fig. 3. Schematic (a) and picture (b) of the two winding probe employed for non-destructive magnetic survey of fiber dispersion.

To this scope, Computational Fluid Dynamics (CFD) approaches are commonly employed, especially implementing (non-Newtonian) single fluid models for the description of the fresh concrete behavior and based on Galerkin FEM discretization of the Navier-Stokes equations, including free surfaces and moving boundaries [73,74].

In order to describe the heterogeneous nature of FRC and its effect on flow-induced heterogeneity/anisotropy, Distinct Element Method (DEM) has been successfully employed [75–78].

The first theoretical basis of the fiber transport problem was laid down in the milestone work by Jeffery [79], who solved the moment equation of a rotating ellipsoid immersed in a Newtonian fluid. The fibers can be considered as infinitely elongated ellipsoid, and their interactions in a semi-dilute/concentrated suspension are suitably described by means of different approaches, among which the most common is the hydro-dynamically induced rotary diffusivity of isotropy [80,81].

In this framework the evolution of a finite group of slender fibers with isotropic initial orientations is considered to represent the macroscopic orientation process. At each time step, the evolution of the orientation of each fiber is directly deduced from the Jeffery equation with the diffusive term of interactions, and the

macroscopic orientation is then calculated as the mean of the orientation of all fibers. The number of chosen fibers is motivated by both a good accuracy of the prediction and the computation time. Applications of industrial interest have been addressed [15,82,83].

Ferrara et al. [84] and Ferrara and Cremonesi [85] have quite successfully attempted to correlate the orientation of the fibers to the direction of the shear rate vectors as predicted by the casting flow simulations. The same approach has been also followed by Orbe et al. [86] who also attempted to correlate the fiber orientation prediction in a full-scale casting geometry (a SFR-SCC wall) to the expectable spatial scattering of the material performance in the hardened state.

A fully coupled approach for the simulation of suspensions of non-Newtonian fluids and rigid particles has been recently proposed by employing the Lattice-Boltzmann method, with its roots in the kinetic theory of gases [87]. The approach treats fluids as individual particles discretized by a set of discrete particle distribution functions and provides rules for the mutual collisions and propagation. The coupled problem of the flow of suspensions of rigid bodies in a non-Newtonian fluid is separated into three levels:

- (i) level of particles, used for dynamics (position and velocities) and interactions of particles (collision and force);
- (ii) level of fluid-particles interaction with particles discretized by Lagrangian nodes and solved by the Immersed Boundary Method; and
- (iii) level of fluid, where the Lattice Boltzmann Method is used for the flow modelling.

The macroscopic quantities can be then computed as moments of the distribution functions.

Successful application of this kind of approach to the simulation of SFR-SCC casting flows and prediction of flow-induced fiber orientation has been recently provided [72].

4. Research outline and significance

Within a comprehensive research effort aimed at developing a holistic approach to the control of execution of structural elements of highly flowable UHPFRC, this paper presents a real case study on HPRCC slabs which have been cast with artificial flow-casting

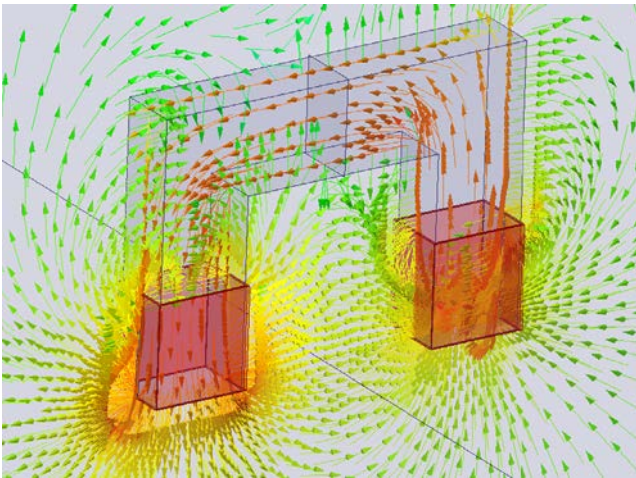


Fig. 4. Two winding probe: flux density predicted by FEM analysis.

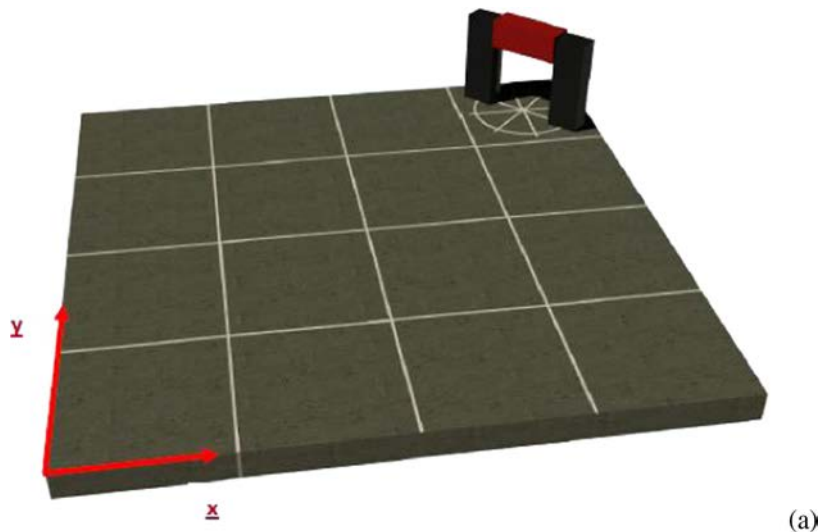


Fig. 5. Schematic of the non-destructive measuring set-up, with x-y reference axes highlighted, (a) and details of the cell schematics employed for each of the investigated HPRCC slabs (b–e) – arrows indicate the pouring points and directions of the fresh HPRCC mixture and solid lines indicate position of prearranged defects.

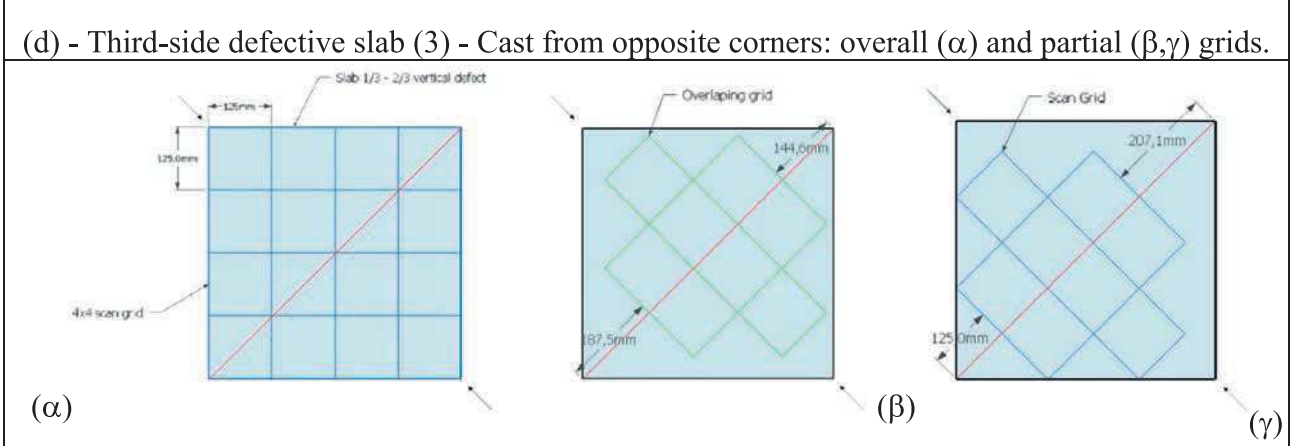
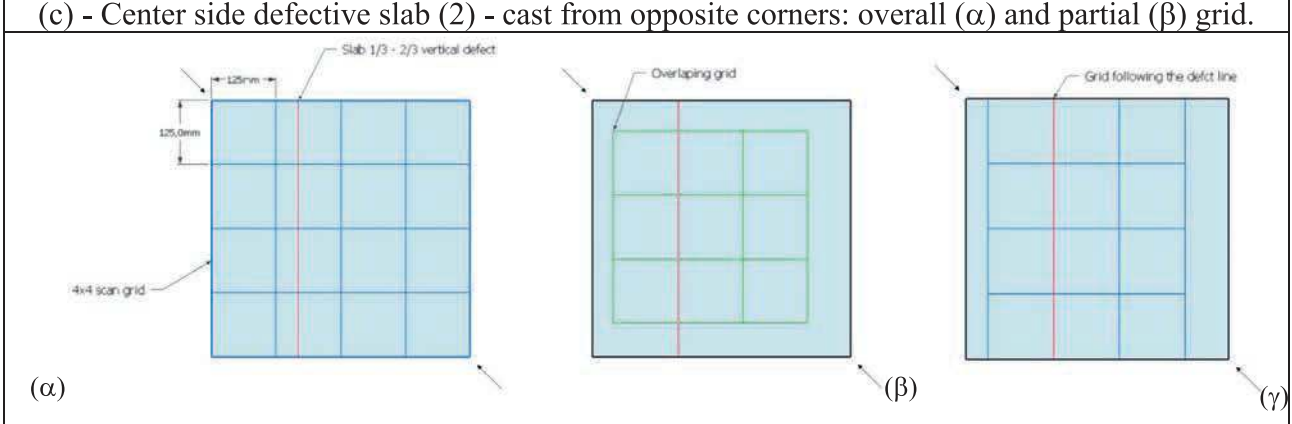
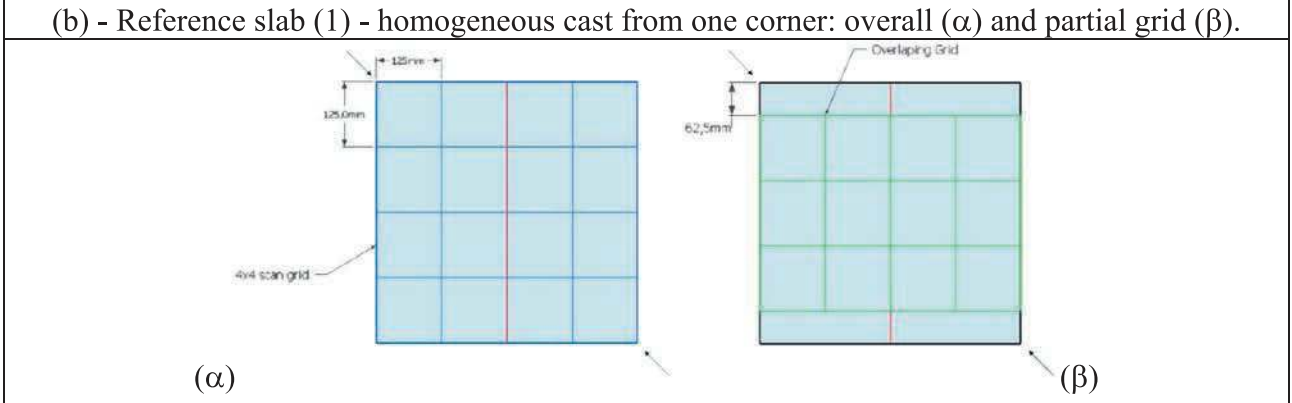
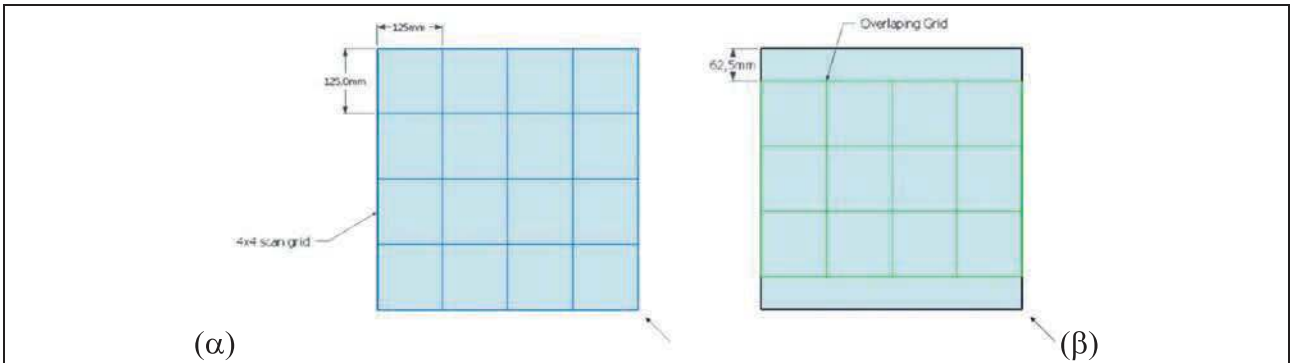


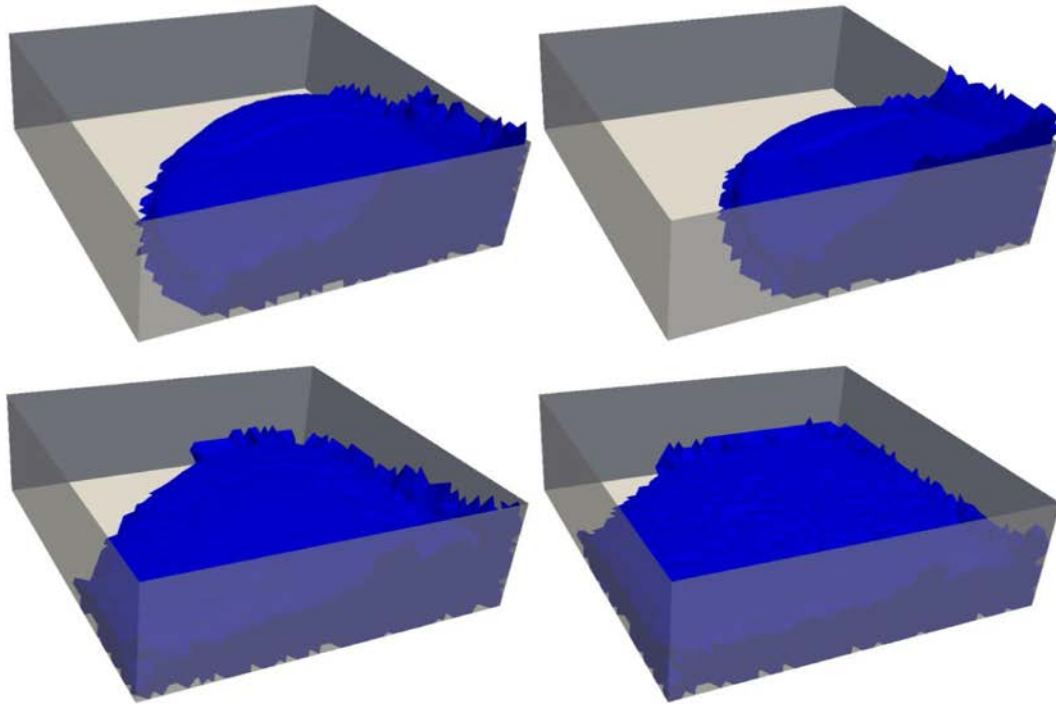
Fig. 5 (continued)

defects, e.g., cold joints or other kinds of “in-structure” physical boundaries, which trigger a strong anisotropy and discontinuity in the flow-induced fiber orientation distribution.

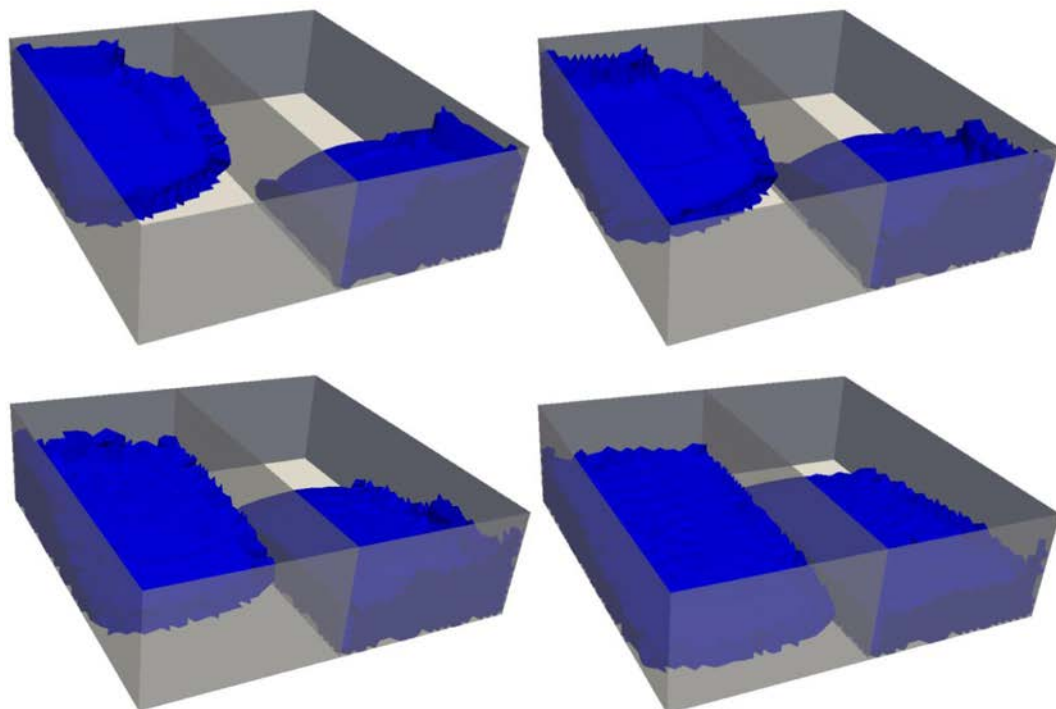
The methodology consists on three steps: firstly, the casting process has been modeled by means of a Computational fluid Dynamics (CFD) modelling tool, employing a Lagrangian approach

based on Particle Finite Element method [88,89], and flow-induced orientation of fibers has been “guessed” through the velocity vector patterns of the simulated casting process.

Secondly, the fiber orientation has been then checked with a non-destructive method, which relies on the effect of the steel fibers on the magnetic properties of the FRCC.

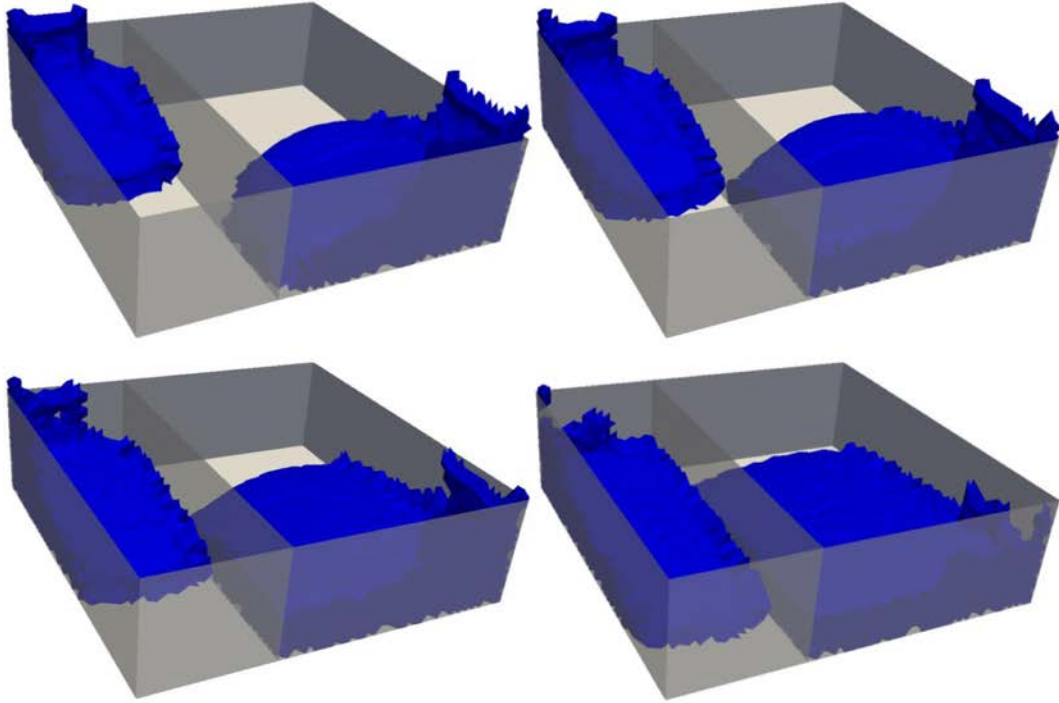


(a) – reference slab with no casting defect

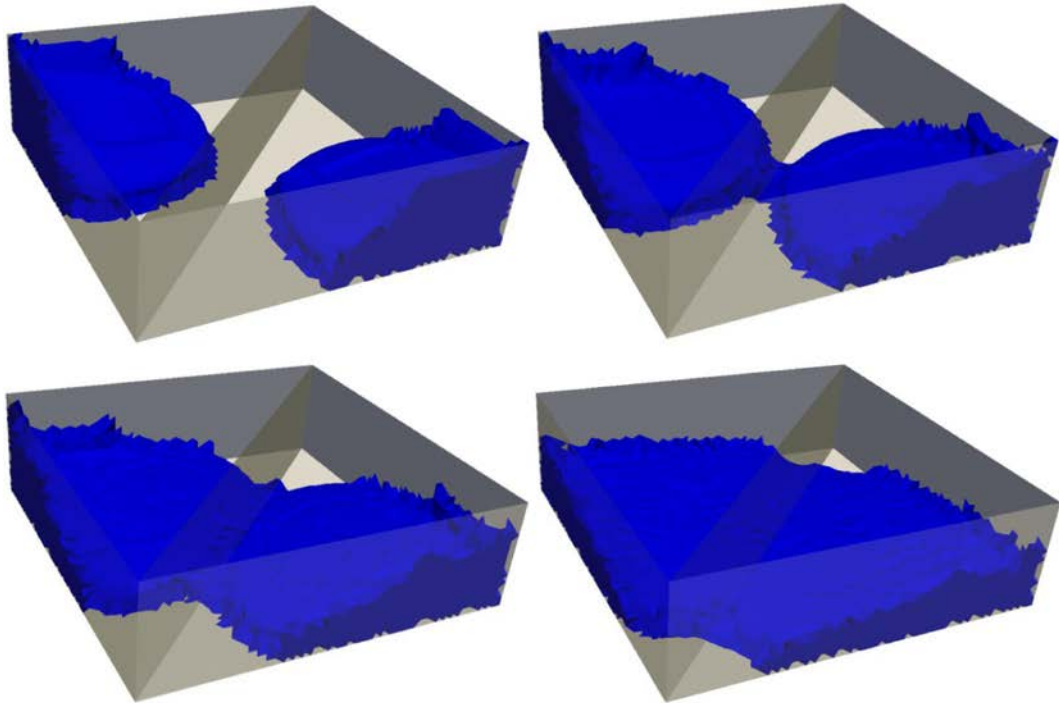


(b) – center side defective slab

Fig. 6. Snapshots of simulated casting processes.



(c)- third side defective slab



(d)- diagonal defective slab

Fig. 6 (continued)

Thirdly, a comprehensive correlation has been established with the cracking process and its development up to failure, as observed in the same slabs when tested under center point load in a suitable configuration (over 8 unilateral supports).

To the authors' knowledge, this work represents one of the first comprehensive throughout applications of the different predictive/monitoring approach with reference to UHPFRC elements. Moreover, it aims at showing how casting flow modelling and

non-destructive survey of fiber dispersion can be usefully exploited as structural design aiding tools in assessing the reliability of anticipated failure modes in structural elements made with highly flowable FRCs, which may be quite sensitive to flow induced orientation of fibers.

5. Experimental program: materials, specimens, CFD prediction and ND fiber monitoring

A commercial UHPFRC (Ductal FM™) has been employed [90], containing 2% by volume of steel fibers, 13 mm long and with a diameter equal to about 0.2 mm and a yielding stress of 2860 MPa.

The UHPFRC was heat cured for 24 h at 90 °C and 100% RH; at 28 days it featured a compressive strength of 198.2 MPa and a Young’s modulus equal to 58.2 GPa. The flexural behavior was also characterized by means of 4-Point Bending Tests (4PBT) on thin beam specimens, with dimensions of 420 mm × 110 mm × 30 mm (span × width × height) according to French recommendations [9].

Square 500 mm side and 30 mm thick slabs were cast, according to four different configurations:

- (i) a slab without defect for which fresh concrete was poured from a corner, letting the flow fill the whole casing (Fig. 1a);
- (ii) a slab with an aluminum divider placed at mid-side (Fig. 1b);

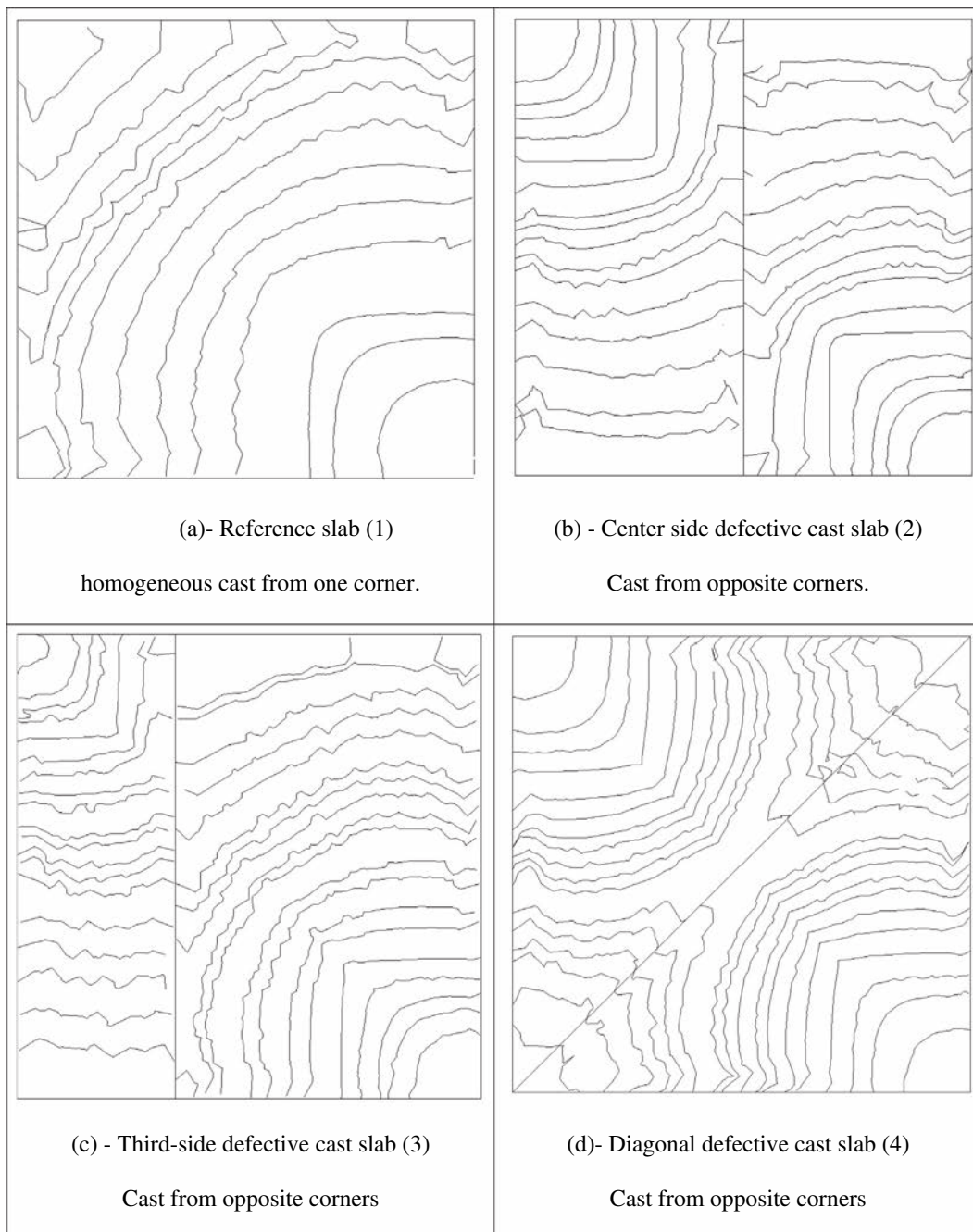


Fig. 7. Envelope lines of the advanced fluid front in simulated casting flow process of the investigated HPRCC slabs. **ctd.:** velocity field vectors in simulated casting processes of the investigated HPRCC slabs.

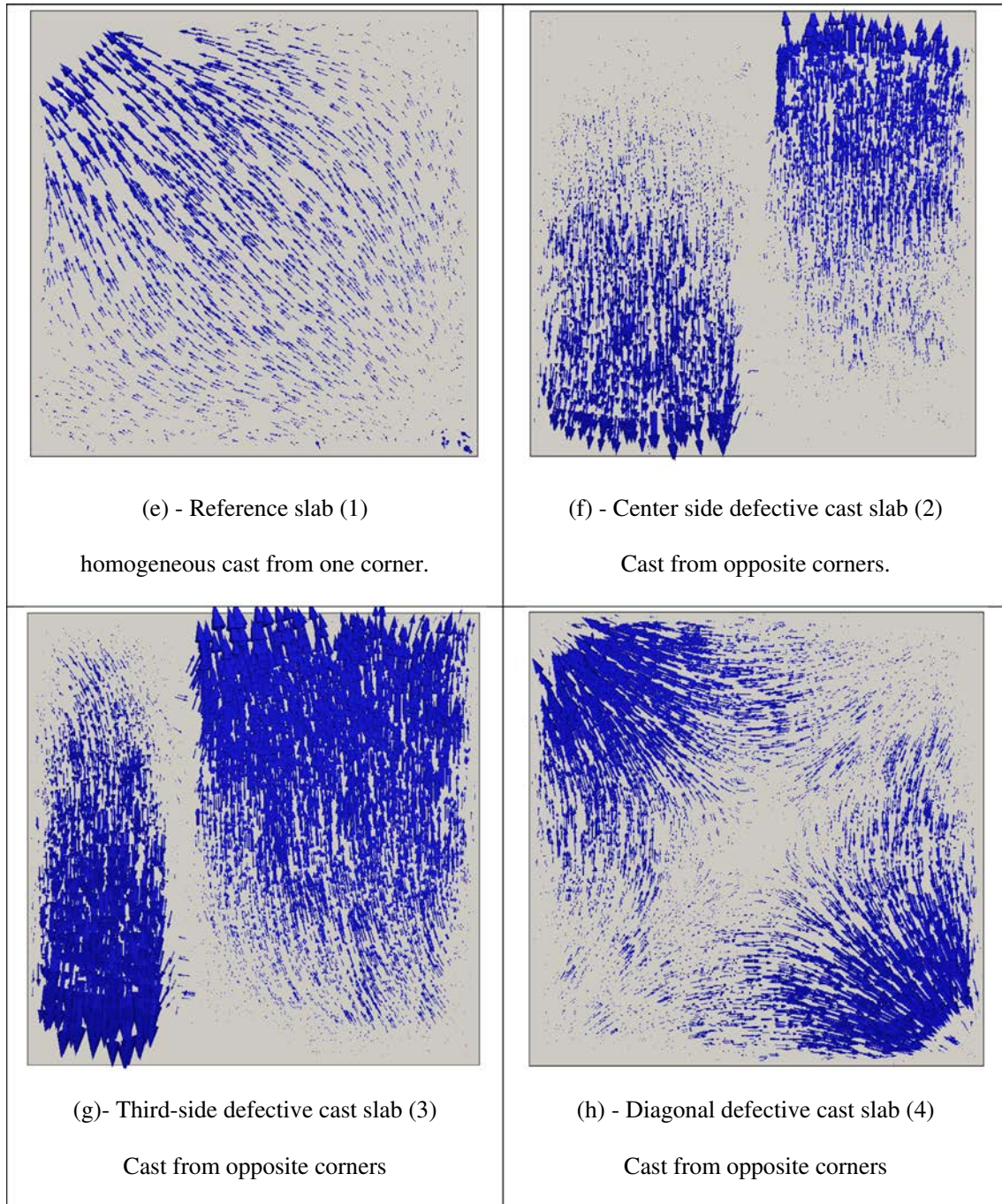


Fig. 7 (continued)

- (iii) a slab with an aluminum divider placed at the side third, the fresh UHPFRC being poured, both in (ii) and (iii) from two opposite corners (Figs. 1c);
- (iv) a slab with a diagonal divider, the fresh UHPFRC being poured from the other two opposite corners (Fig. 1d).

The aluminum divider was removed once the fresh concrete was fully cast in place, causing a strong discontinuity in the fiber distribution in the divider line, which may somehow represent a cold joint in real casting. Different colorants (brown and grey) were added to the mixtures, in order to distinguish the concrete cast from either corner.

The casting process of all the four investigated slabs was simulated with a Computational fluid Dynamics (CFD) model, employ-

ing a Lagrangian approach based on Particle Finite Element method, the detailed formulation of which has been described in [25,29]. The flow chart in Fig. 2 summarizes the main steps of the approach. A re-meshing tool, based on maximum element distortion index, was implemented for an effective description of the free surface flow problem [89].

The employed HPFRCC has been modeled as a Bingham fluid with $\tau_0 = 20$ Pa and $\mu = 100$ Pa s, as from previous investigations on the rheology of this kind of cementitious composites [91,92].

Coherently with the approach adopted by the first author in [84], information about fiber orientation could be correlated to the direction of the flow velocity vectors in the simulated casting domain. This approach, though simplified, is able to provide the information about the trend of spatial orientation of fibers in the

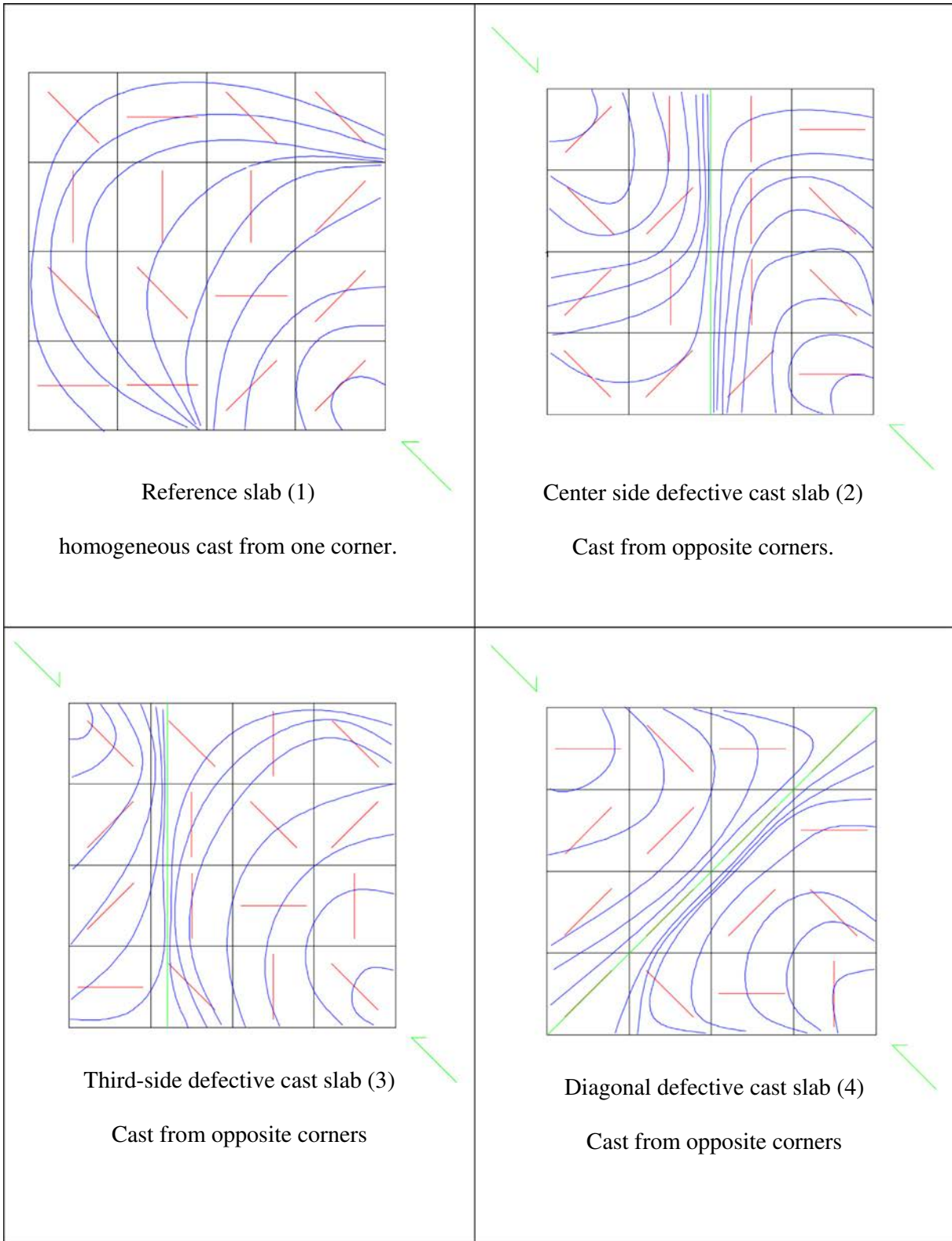


Fig. 8. Matching between directions of maximum measured compensated inductance (red segments) and simulated advance of casting flow front for the four investigated HPRCC slabs. (For interpretation of the references to colour in this figure legend, the reader is referred to the web version of this article.)

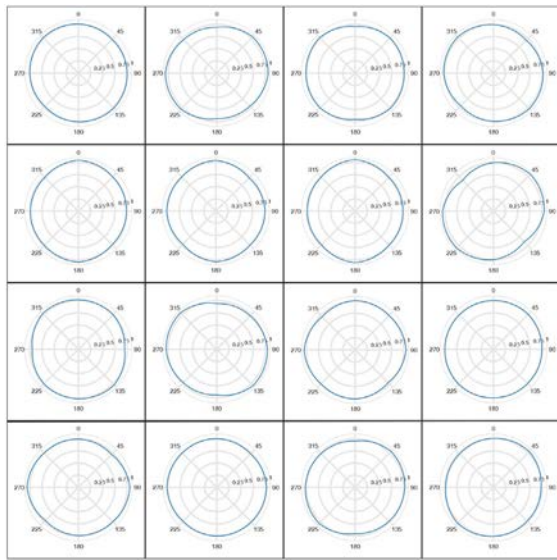
structural element as cast which may be sufficient for structural applications such as the ones herein dealt with. It is worth remarking that the benefits of fibers are best exploited in a structural configuration allowing for sufficient redistribution of post-cracking stresses, as the slabs here tested. In these cases “local” or “point-

wise” information about fiber concentration and orientation may be redundantly detailed, since right the aforementioned stress redistribution capacity would allow to shadow concentrated defects, still remaining sensitive to a major “average spatial” trend in spatial dispersion and orientation of the fibers.

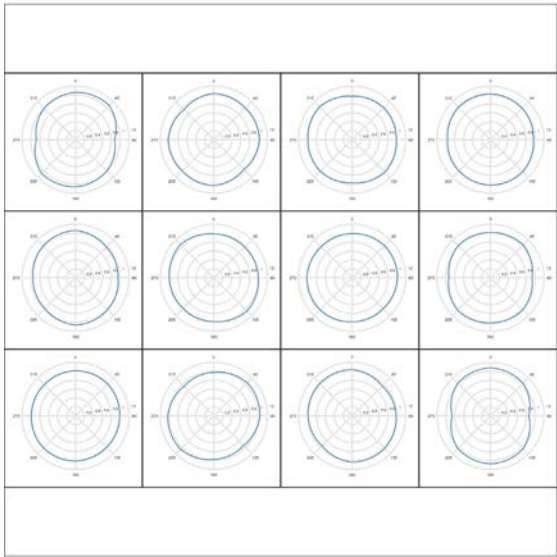
Non-destructive monitoring of fiber dispersion and orientation was performed on the slabs, once hardened, according to the methodology proposed in [71,19], and hereafter briefly summarized.

The employed set-up is shown in Fig. 3, which consists of a C-shaped ferrite core with two windings: the first one generates the magnetic field, while the second is employed to pick up the induced electromotive force. The excitation winding is split into two coils which are wound around each leg of the probe. This arrangement is likely to increase the fraction of the magnetic flux linked with the coils which hits the material under test. The sense winding is placed over a coil of the excitation winding in order to reduce the leakage reactance. Fig. 4 shows the flux density

predicted by FEM magneto-static analysis. The measurement of the electromotive force induced in the pickup winding and of the current flowing through the excitation winding allows the losses due to the alternating magnetic field to be directly estimated. However, it is still not possible to separate the power losses due to the steel fibers from those due to the ferrite core. Under the assumption that the flux density in the core would not be affected by the presence of the steel fiber, the power losses due to steel fibers only could be estimated by evaluating the power losses when the probe is laid on the specimen and subtracting those measured when it is placed away from ferromagnetic objects. Nonetheless, since the ferromagnetic behavior of the steel fibers in the specimen increases the flux density in the core, the increase of

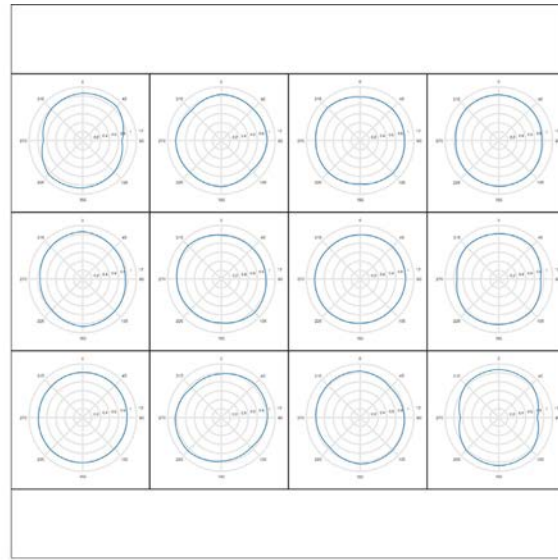


(α)

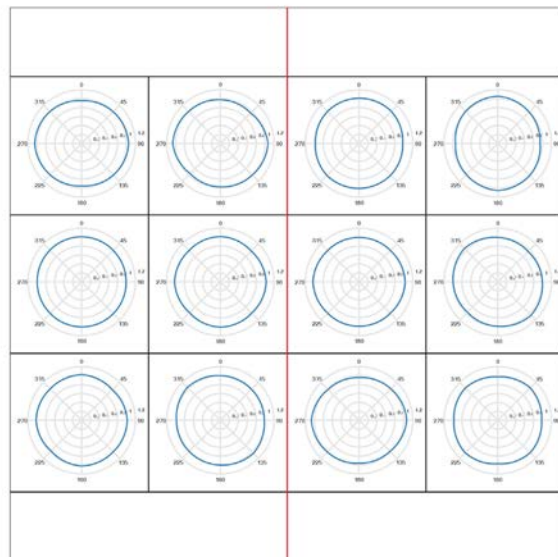


(β)

(a) -Reference slab (1) - homogeneous cast from one corner : overall (α) and partial grid (β).



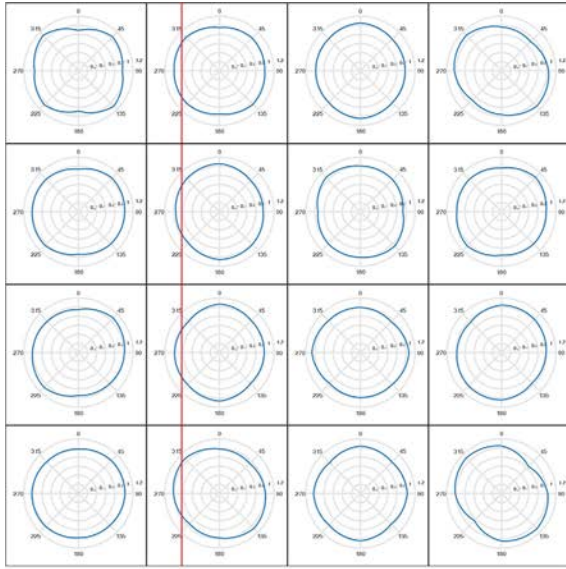
(α)



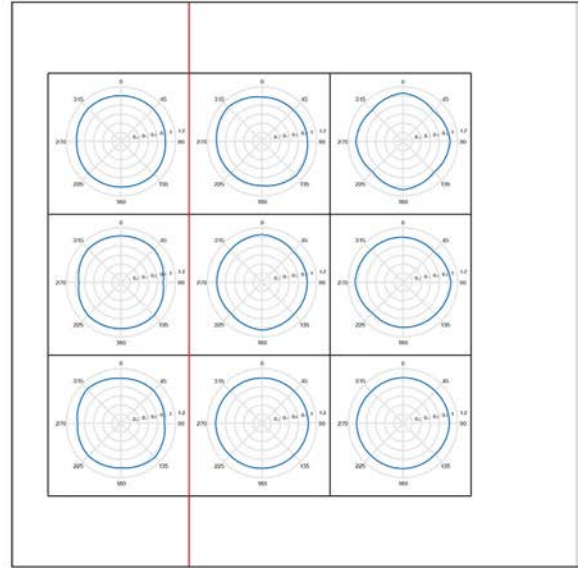
(β)

(b) - Center side defectiveslab (2) - cast from opposite corners: overall (α) and partial (β) grid.

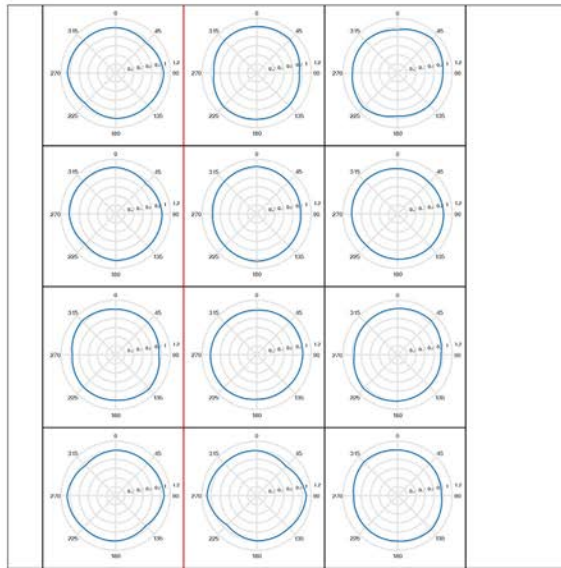
Fig. 9. Polar plots of local anisotropies in fiber orientation as from non-destructive magnetic survey for the four investigated HPFRCC slabs.



(α)



(β)....



(γ)

(c) -Third-side defectiveslab (3) - Cast from opposite corners: overall (α) and partial (β,γ) grids.

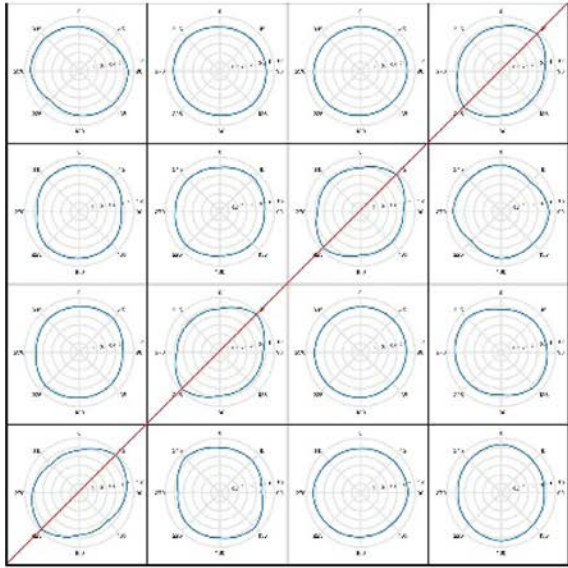
Fig. 9 (continued)

the power losses due to the alternating magnetic field which is measured when the probe is placed on a SFRC specimen is only partially related directly to the losses occurring in the steel fibers, while the rest is caused by the increase of the core losses [71].

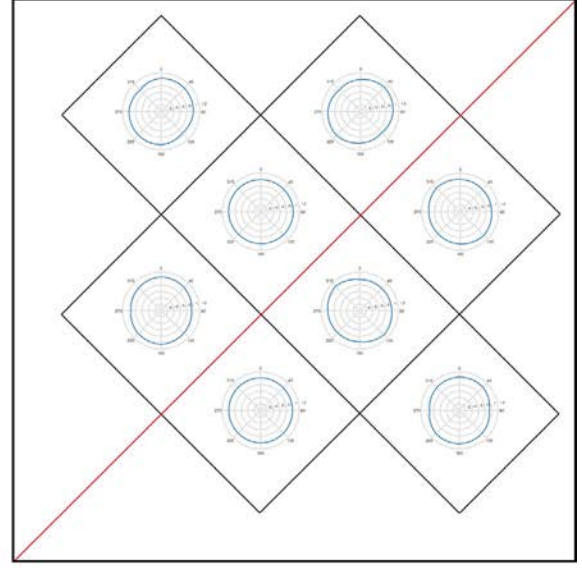
In order to avoid this problem, the sense winding has been employed to set up a proper feedback controller which imposes the voltage across it, hence its flux linkage. In this case the variation of the flux density in the ferrite core due to the steel fibers can be minimized, which furthermore results in minimized core losses. Thanks to the two-winding probe with a closed loop set-up, the difference between the losses due to the alternating

magnetic field when the probe is placed on the specimen and those evaluated when it is placed away from any ferromagnetic material provides a good estimate of the power losses occurring in the steel fibers alone.

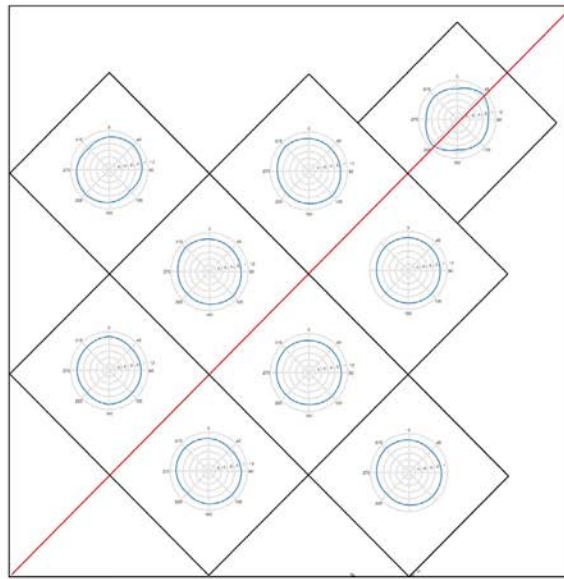
The measurement procedure is extremely simple: the probe is laid on the surface of the specimen, and the evaluation of the inductance is performed. Its value is clearly affected by both the fiber concentration and orientation in the specimen. The dependence on fiber concentration can be easily understood considering that the presence of steel fibers increases the effective magnetic permeability of the composite material according to a simple



(α)



(β)



(γ)

(d) - Diagonal defective slab (4) - Cast from opposite corners: overall (α) and partial (β, γ) grids.

Fig. 9 (continued)

mixture rule, and, e.g., the impedance measured at the terminals of the equivalent electrical circuit can be expressed as:

$$Z = R_c + j\omega[L_l + L_v] \quad (2)$$

where R_c denotes the resistance of the coil and L_l and L_v respectively denote the magnetic inductance associate to a magnetic flux outside and through the specimen. The inductance L_v can be split into a matrix contribution L_{v0} and an incremental contribution $\Delta L_{v, \text{fibers}}$, denoted as compensated inductance henceforth, which depends on the fiber volume fraction and orientation. Whereas inductance L_v depends on the measurement frequency, compensated inductances results independent of it [70,71,19].

The procedure to assess the effect of the fiber orientation has to take into account that the electromagnetic properties of the composites, as remarked above, become anisotropic (dyadic) if the fibers are not randomly oriented. In case of a preferential alignment of the fibers, by rotating the probe on the specimen and measuring the inductance along different directions, a dependence of the measured inductance on the probe orientation will be detected: the direction along which the maximum value of the inductance is measured will most likely coincide with the preferential alignment of the fibers. The magnitude of the inductance variation is correlated to the degree of orientation of the fibers.

The UHPFRC slabs were analyzed according to different "cell-schematics" as shown in Fig. 5, measurements in each cell being

taken along four different directions, namely at 0°, 45°, 90° and 135° to a reference y-axis. For each direction measurements were repeated four times, and reference will be made henceforth to the average of the four thus garnered values. Arrows in Fig. 5 indicate the direction of casting, whereas the solid thicker line indicates the pre-arranged discontinuity. The choice of the measuring grids was dictated by the geometry of the slab and by the position of the casting defect, as well as by the need of garnering information on fiber dispersion and orientation also across the same casting defects as above.

Quantitative assessment of local concentration of fibers, for each of the measured slab cells, was performed through the calibration of the relationship between the “nominal average compensated inductance” and the nominal “design” fiber content in the mix. The former is defined as the average, computed over the whole slab, of the averages of the compensated inductance as

measured along the four directions for each cell. By means of such a calibrated law, the average values of compensated inductance for each cell could be processed to assess whether and to what extent the local concentration of fibers differed from the assumed nominal value. For the assessment of fiber orientation, “fractional” compensated inductances along each direction α were calculated as:

$$f_\alpha = \frac{\Delta L_\alpha}{0.25(\Delta L_0 + \Delta L_{45} + \Delta L_{90} + \Delta L_{135})} \quad (3)$$

6. Casting flow simulations

Fig. 6a–d shows some significant snapshots of the simulated casting processes for all the four investigated slabs. The iso-velocity lines for advancing flow front along the simulated flow

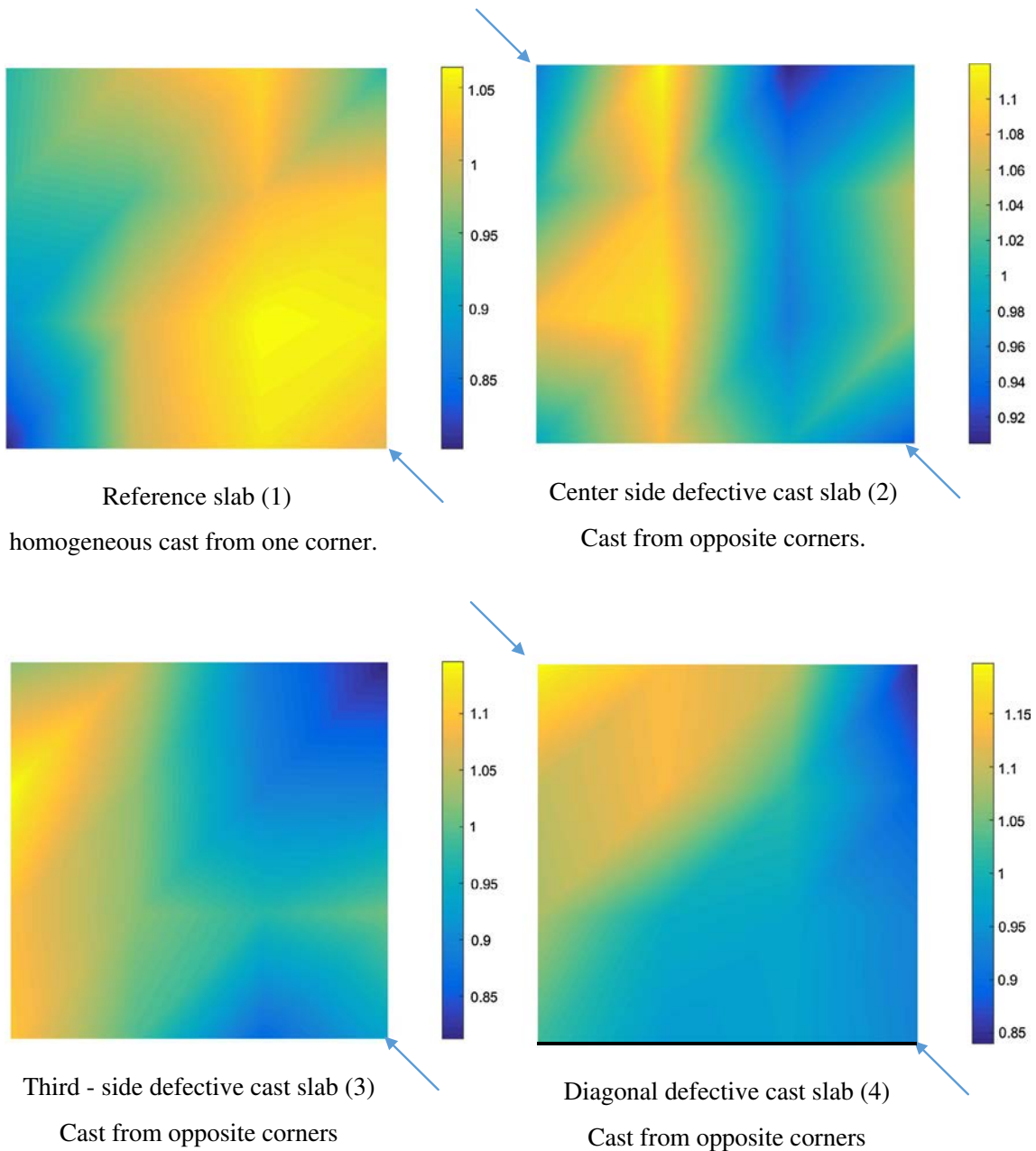


Fig. 10. Estimation of homogeneity in fiber distribution content in the four investigated HPRCC slabs – values of the homogeneity parameter higher/lower than 1 will indicate fiber content higher/lower than nominal reference one – arrows indicate pouring points and directions.

processes as well as the velocity field vectors were obtained, as shown in Fig. 7a–d and e–h respectively. The envelope lines represent the advancement of the fluid front along the casting process, transporting and aligning the immersed fibers. They are going to be correlated to the orientation of the fibers, as assessed through the non-destructive magnetic survey in the forthcoming section.

7. Non-destructive magnetic surveyed fiber dispersion and orientation

As preliminary information obtainable from the non-destructive survey of fiber dispersion and orientation, the

directions have been plotted (Fig. 8a–d) along which the maximum values of compensated inductances have been measured (as from the schematics in Fig. 5). The aforementioned directions (red segments in Fig. 8) do correspond fairly well to the computed flow streamlines which model the advancement of the free flow front in the simulated casting process. This is also in agreement with previous literature findings, for which in a free casting flow fibers tend to align parallel to the free edges of the same flow [31,49,78].

In Fig. 9a–d, polar plots of the fractional compensated inductances allow to have a deeper insight into the degree of anisotropy in fiber dispersion, caused by the casting flow process as by the prearranged geometrical discontinuities, in case. As a matter of fact the fractional compensated inductance represents a measure of

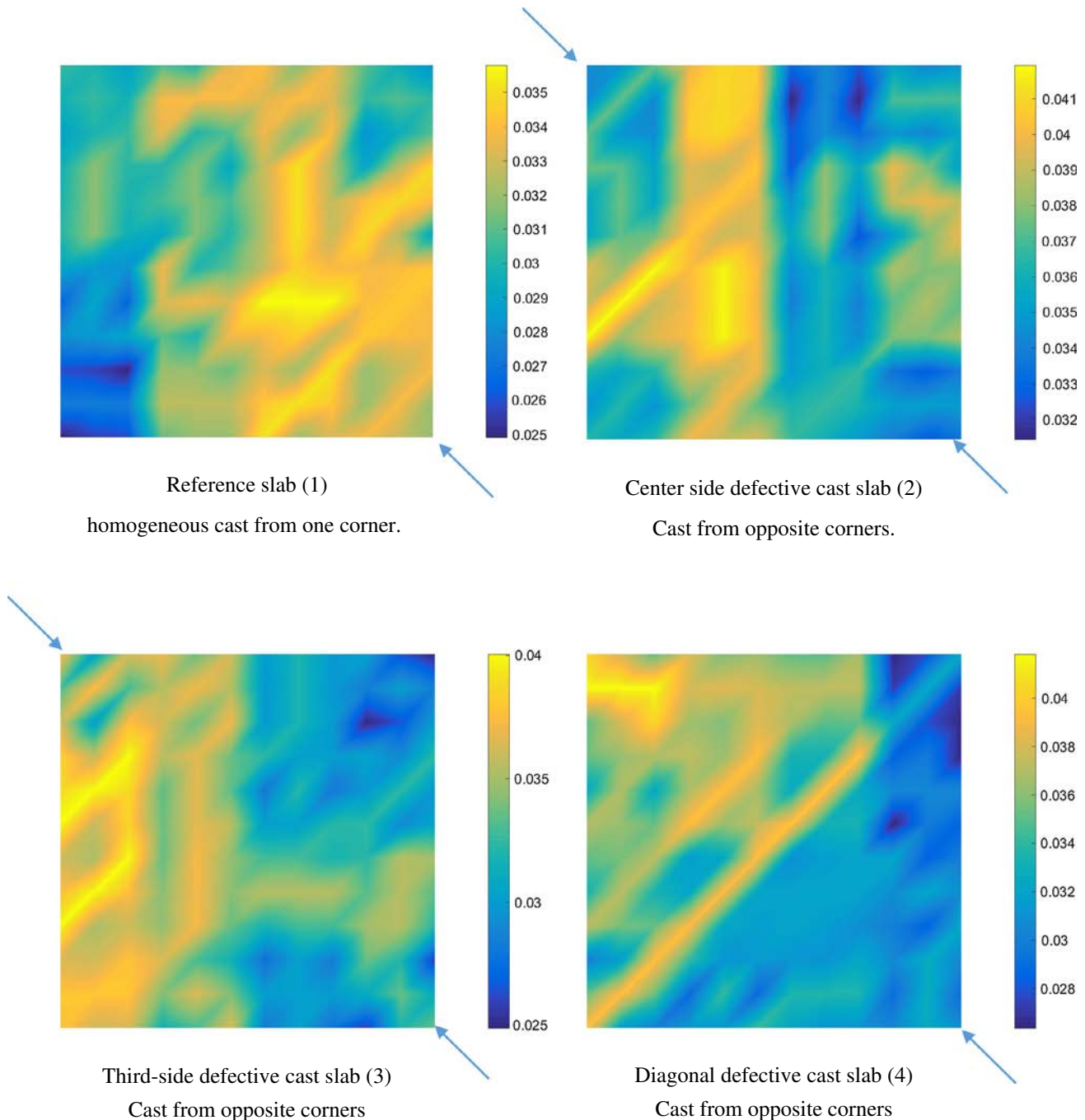


Fig. 11. Estimation of homogeneity in fiber distribution content and orientation in the four investigated HPFRCC slabs – higher values of the compensated inductance indicate higher concentration of fibers along the plotted direction – arrows indicate pouring points and directions.

how much the inductance measured along one direction exceeds the average isotropic value and hence is an effective measure of the fiber dispersion anisotropy.

It can be observed that in the reference slab without any geometrical discontinuity a substantially isotropic dispersion has been obtained, with some moderate deviations most likely due to wall effects along the boundaries. On the other hand, in the slabs with a geometrical discontinuity, either parallel to the side or diagonally arranged, the fiber dispersion features evident anisotropy because of the wall effect provided by the discontinuity. Interestingly the anisotropy is better detected when the sensor is placed across the discontinuity (Fig. 9a–d).

Fig. 10a–d provide information about local fiber concentration, in the form of “iso-quantity” curves, as explained in detail in Section 3. Such quantitative information is obtained by calculating the average value of the four measurements garnered in each single cell and normalizing it by the average of the averages, referring to the structural element as a whole. The latter quantity can be regarded as an indicator of the nominal content of fibers inside the structural element. Zones where the value of such a normalized local average compensated inductance is higher than one thus will indicate zones with potentially higher local concentration of fibers.

From plots in Fig. 10a–d, the following observations can be drawn:

- the degree of homogeneity of fiber concentration inside each single slab is quite good, observed deviations always falling in the range $\pm 10\text{--}15\%$;
- in the reference slab, diagonally cast from one single corner and with no geometrical discontinuity inside, the aforementioned heterogeneity is evidently due to dynamic segregation of the fibers along the casting direction, as well as to some corner effects;
- in the slabs with prearranged defects, the effect of dynamic segregation of the fibers is less strong, most likely because of the lower distance travelled by the casting flow. On the other hand a sensible difference between the two “halves” of the slab appear: the half which was cast as the former being always poorer, in fiber content, than the latter, which was cast only

once the former was completed. This fact can be justified by invoking some static segregation which may have occurred in the bucket employed to cast the slabs, which made richer in fibers the portion of the bulk material which was poured later in the molds.

Information about local fiber concentration and orientation has been jointly plotted in Fig. 12a–d, where the local compensated inductances, along each of the four surveyed directions in each cell, have been weighed by the concentration homogeneity factor, as above in Fig. 10a–d. This allows having an output of immediate graphical significance, which indicates in a clear way where a larger concentration of fibers could be expected and along which direction.

8. Comparison between fiber dispersion patterns and crack patterns

As a final check, which also stands as a proof of the significance of the whole performed investigation, a comparison has been attempted between the fiber dispersion patterns, as in Fig. 10a–d, and the cracking patterns obtained when testing the same surveyed slabs under center point load, according to the schematic set-up shown in Fig. 11.

Crack patterns have been surveyed by means of a dedicated Digital Image Correlation (DIC) set-up and system, described in detail in [90,93], where also information about the results of mechanical tests can be found.

Crack patterns, as evolving along the loading path and up to failure, are shown in Fig. 13a–d, and superimposed to fiber concentration and orientation patterns in Fig. 14a–d.

Besides the clear influence of the prearranged discontinuity, at least in two of the three investigated cases featuring it, a systematic agreement between the directions of the main cracks and those featuring the highest concentration and most favorable orientation of fibers can be observed. That is, the cracks formed orthogonally to the direction of weakest post-cracking performance of the material, which is that of least favorable orientation

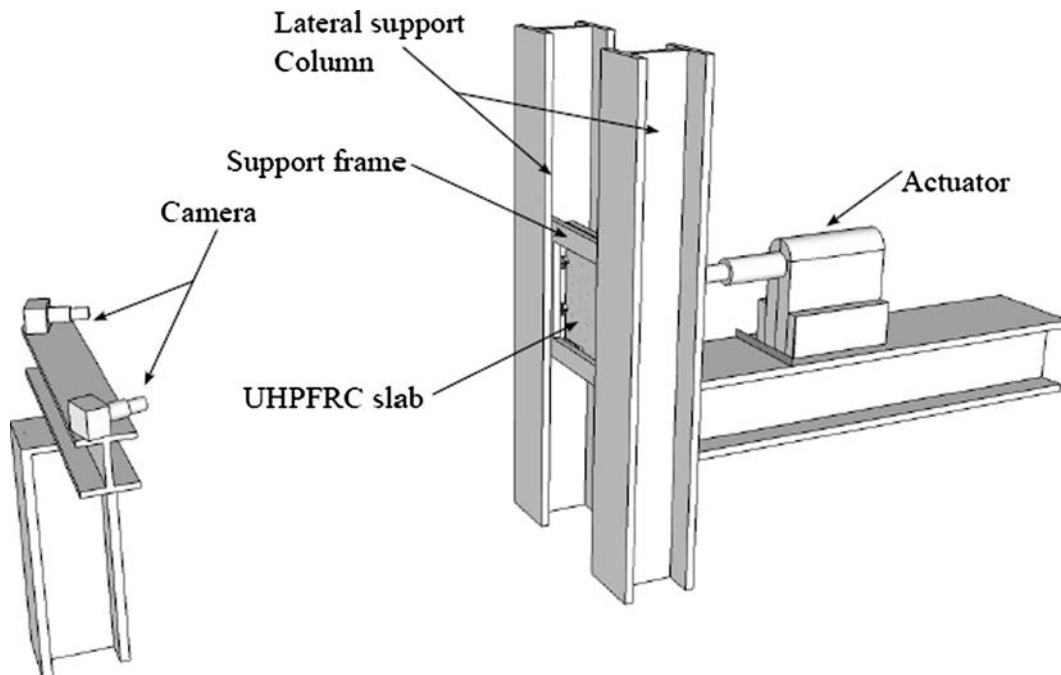
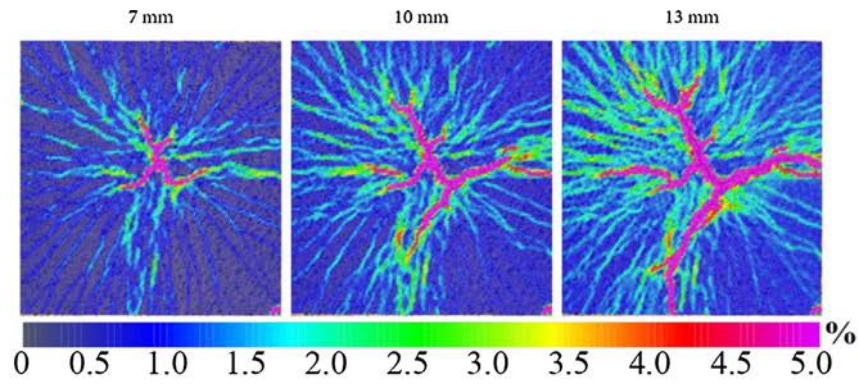
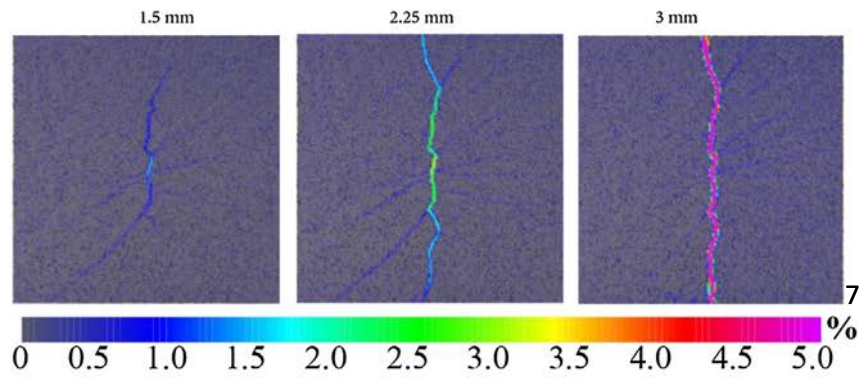


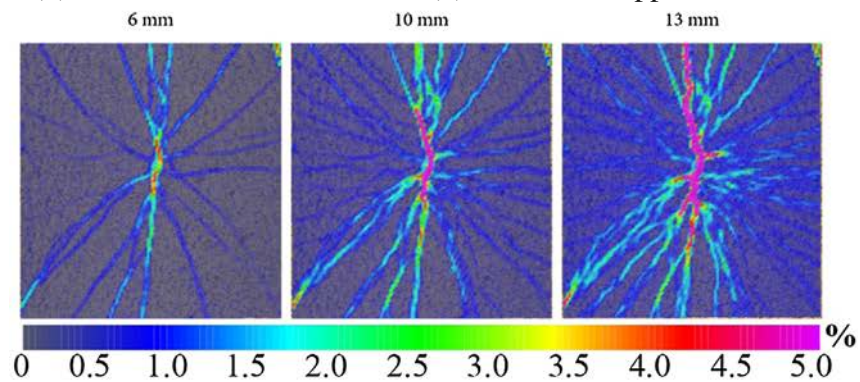
Fig. 12. Schematic of the test set-up and stereo-vision digital image correlation system employed for mechanical tests on surveyed UHPC slabs.



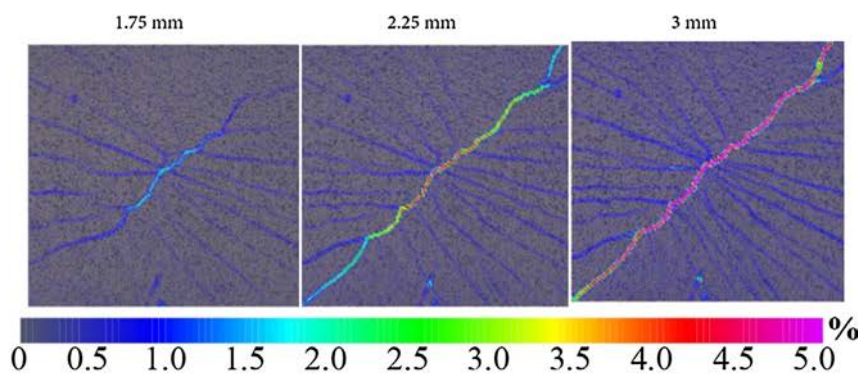
(a) - Reference slab (1) - homogeneous cast from one corner.



(b) - Center side defective slab (2) - cast from opposite corners.

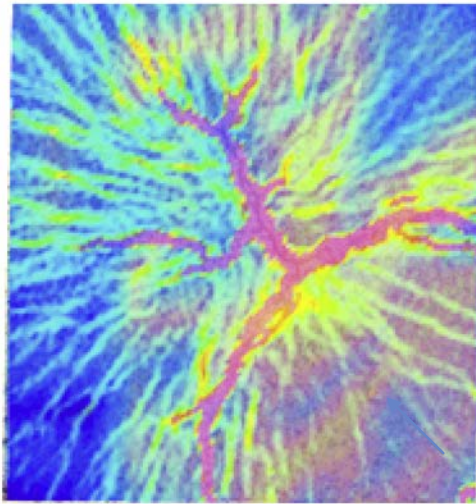


(c) - Third-side defective slab (3) - cast from opposite corners.



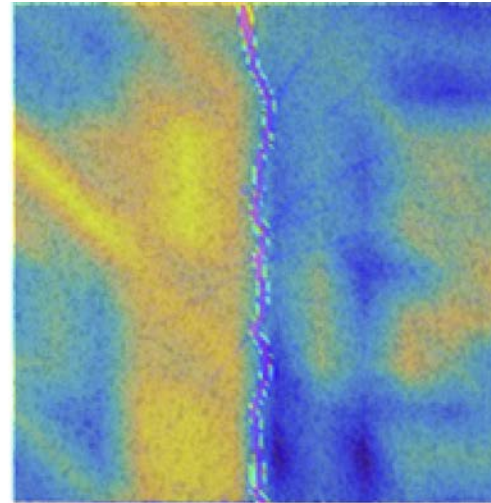
(d) - Diagonal defective slab (4) - Cast from opposite corners.

Fig. 13. Evolution of crack and deformation patterns during load tests for the four investigated HPFRCC slabs.



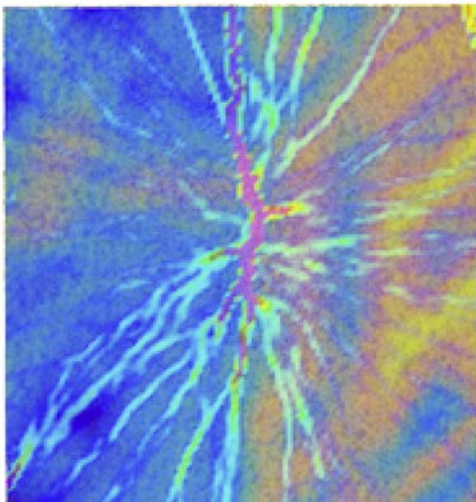
Reference slab (1)

homogeneous cast from one corner.



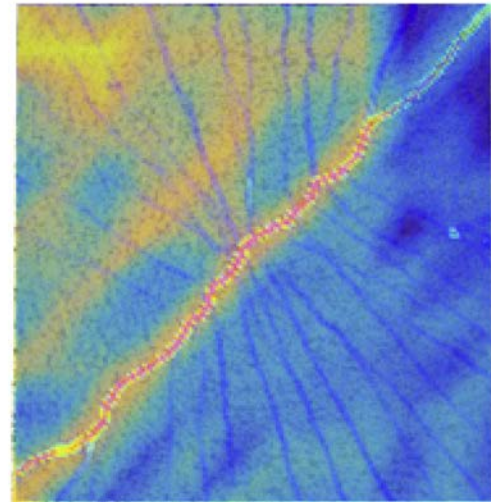
Center side defective cast slab (2)

Cast from opposite corners.



Third - side defective cast slab (3)

Cast from opposite corners



Diagonal defective cast slab (4)

Cast from opposite corners

Fig. 14. Superposition between fiber dispersion and homogeneity plots and crack patterns at failure for the four investigated HPRCC slabs.

of the fibers. Moreover, and quite more interestingly, front of dynamic segregation, i.e. zones in the slab where a steeper decrease in local fiber concentration was observed, highlighted by the sharpness and narrowness in color scale renderings, also acted both as a defect and as an arresting front for the cracks, which hence tended to propagate parallel to it.

This is evident in the case of the reference slab with no defect, where fibers dispersion was quite isotropic as only slightly affected by some degree of dynamic segregation of the same fibers starting from the casting corner. The main cracks evidently developed following, as above said, with the front of dynamic segregation (Fig. 13a). With reference with the slab with the casting defect at 1/3 of the side the evidence of the casting defect on failure mode is less immediate. As a matter of fact, though the major crack did not followed the casting defect boundary, the presence of the last

only allowed one major longitudinal crack to localize. Moreover the radial micro-cracks developed asymmetrically, with clear evidence of the zone where larger concentration of fibers was detected and where larger post-cracking stress redistribution was allowed.

The matching between weak crack plane and the measured fiber orientation confirms thus the reliability of the non-destructive fiber dispersion monitoring approach.

This highlights once again the importance of coherently “incorporating” flow-induced orientation of the fibers in the structural design of elements made with highly flowable HPRCCs. This can be accomplished either through a “one-parameter” approach, such as the K-factor one proposed by *fib* Model Code 2010 [8,9] or with advanced approaches which make explicit reference to an “in-structure monitored” orientation of the fibers. The latter, on its

hand, can be accounted for in a deterministic way, with reference only to the main fiber alignment, as this study would pave the way for, as well as through more refined probabilistic fiber orientation distributions [39,40].

9. Concluding remarks

The coherence between the presented results in term of magnetic inductance, simulated fiber orientation and crack patterns as measured using digital image correlation corroborate the reliability of the proposed approach. It also confirms that a single fluid approach can be reasonably employed to the aforementioned purpose, i.e., fiber alignment being predictable via the modeled field of the shear rate vector. Furthermore, the combined analyses have coherently confirmed flow-induced orientations of fibers in free casting flows.

Fiber concentration/orientation patterns, as obtained from the ND-magnetic survey, and crack patterns, observed on the slabs tested under center point load, matched satisfactorily, thus confirming the role of uneven fiber dispersion in governing the failure mode. The aforementioned comparison has also shown that dynamic segregation of fibers may represent sites for potential crack localization.

This study showed the powerfulness of a holistic design approach which incorporated on CFD modelling and ND monitoring for structural elements made with highly flowable HPRCCs, i.e., a tool for assessing the effect of fiber dispersion on the performance of hardened structural elements made of highly flowable HPRCCs as affected by the tailored casting process. The approach has to be completed with the development of orthotropic constitutive laws for the material, which could be calibrated on the results obtained from CFD prediction and ND fiber survey. This opens the possibility of not only predicting but also optimizing casting flow process of highly flowable HPRCCs with respect to the structural applications.

Acknowledgements

The authors acknowledge the financial support of the National Sciences and Engineering Research Council of Canada (NSERC) funding – Collaborative Research and Development Grants (RDCPJ 445200). The authors are also grateful to Mr. Gabriele Mero and Mr. Gregorio Nicol Villirillo, who performed the non-destructive survey of fibre dispersion, in partial fulfilment of the requirements for the achievement of their BEng in Civil Engineering at Politecnico di Milano.

References

- [1] Kunieda M, Rokugo K. Recent progress on HPRCC in Japan: required performance and applications. *J Adv Concr Technol* 2006;4(1):19–33.
- [2] Graybeal B. Structural behavior of ultra-high performance concrete prestressed I-girders FHWA-HRT-06-115. Washington, DC: Department of Transportation, Federal Highway Administration; 2006. p. 104.
- [3] Graybeal B. Structural behavior of a prototype ultra-high performance concrete Pi-girder NTIS Report No. PB2009-115495. Washington, DC: U.S. Department of Transportation, Federal Highway Administration; 2009. p. 145.
- [4] Aitcin PC, Lachemi M, Adeline R, Richard P. The Sherbrooke reactive powder concrete footbridge. *Struct Eng Int* 1998;2(8).
- [5] Vicenzino E, Culham G, Perry VH, Zakariassen D, Chow TS. First use of UHPFRC in thin precast concrete roof shell for Canadian LRT station. *PCI J* 2005;(Sept-Oct):50–67.
- [6] Walraven J. High performance fiber reinforced concrete: progress in knowledge and design codes. *Mater Struct* 2009;42:1247–60.
- [7] Sorelli L, Toutlemonde F. Finite element modelling of FRC/UHPFRC in support of innovative structural applications. In: *Proceedings of the 3rd international conference on construction materials: performance, innovations and structural implications*, CONMAT-05, Vancouver, Canada, August 22–24; 2005.
- [8] fib Model code 2010; 2012, 2 volumes.

- [9] Toutlemonde F, Resplendino J, editors. *Designing and building with UHPFRC: state of the art and development* ISBN: 978-1-84821-271-8, hardcover. London-New York: Wiley-ISTE; 2012. p. 814.
- [10] Bayasi MZ, Soroushian P. Effect of steel fiber reinforcement on fresh mix properties of concrete. *ACI Mater J* 1992;89(2):369–74.
- [11] Ferrara L, Meda A. Relationships between fibre distribution, workability and the mechanical properties of SFRC applied to precast roof elements. *Mater Struct* 2006;39(4):411–20.
- [12] Ferrara L, Park YD, Shah SP. Correlation among fresh state behaviour, fiber dispersion and toughness properties of SFRCs. *ASCE J Mater Civil Eng* 2008;20(7):493–501.
- [13] Stahl P, Custer R, van Mier JGM. On flow properties, fibre distribution, fibre orientation and flexural behaviour of FRC. *Mater Struct* 2008;41(1):189–96.
- [14] Ferrara L, Ozyurt N, di Prisco M. High mechanical performance of fiber reinforced cementitious composites: the role of “casting-flow” induced fiber orientation. *Mater Struct* 2011;44(1):149–68.
- [15] Martinie L, Roussel N. Simple tools for fiber orientation prediction in industrial practice. *Cem Concr Res* 2010;41:993–1000.
- [16] Toutlemonde F, Sercombe J, Torrenti JM, Adeline R. Développement d'un conteneur pour l'entreposage de déchets nucléaires : résistance au choc. *Revue Française de Génie Civil* 1999;3(7–8):729–56.
- [17] Grunewald S. Performance based design of self compacting steel fiber reinforced concrete. Delft University of Technology; 2004 [PhD thesis].
- [18] Toutlemonde F. *Contribution à la connaissance et à la maîtrise de quelques non-linéarités du comportement mécanique des bétons et de leur effet sur le fonctionnement des structures, assortie de quelques réflexions méthodologiques. Etudes et recherches des LPC, OA42; 2004.*
- [19] Ferrara L, Faifer M, Muhaxheri M, Toscani S. A magnetic method for non destructive monitoring of fiber dispersion and orientation in Steel Fiber Reinforced Cementitious Composites – part 2: correlation to tensile fracture toughness. *Mater Struct* 2012;45(4):591–8.
- [20] Orbe A, Cuadrado J, Losada R, Rojí E. Framework for the design and analysis of steel fiber reinforced self-compacting concrete structures. *Constr Build Mater* 2012;35:676–86.
- [21] Ferrara L, Bamonte P, Caverzan A, Musa A, Sanal I. A comprehensive methodology to test the performance of Steel Fibre Reinforced Self-Compacting Concrete (SFR-SCC). *Constr Build Mater* 2012;37:406–24.
- [22] Abrishambaf A, Barros JAO, Cunha VMCF. Relation between fibre distribution and post-cracking behaviour in steel fibre reinforced self-compacting concrete panels. *Cem Concr Res* 2013;51:57–66.
- [23] di Prisco M, Ferrara L, Lamperti MGL. Double Edge Wedge Splitting (DEWS): an indirect tension test to identify post-cracking behaviour of fibre reinforced cementitious composites. *Mater Struct* 2013;46(11):1893–918.
- [24] Sanal I, Ozyurt Zihnioglu N. To what extent does the fiber orientation affect mechanical performance? *Constr Build Mater* 2013;44:671–81.
- [25] Orbe A, Rojí E, Losada R, Cuadrado J. Calibration patterns for predicting residual strengths of steel fibre reinforced concrete (SFRC). *Compos – Part B: Eng* 2014;58:408–17.
- [26] Pujadas P, Blanco A, de la Fuente A, Cavalaro SHP, Aguado A. Multidirectional double punch test to assess the post-cracking behaviour and fibre orientation of FRC. *Constr Build Mater* 2014;58:214–24.
- [27] Pujadas P, Blanco A, de la Fuente A, Cavalaro SHP, Aguado A. Fibre distribution in macro-plastic fibre reinforced concrete slab-panels. *Constr Build Mater* 2014;64:496–503.
- [28] Švec O, Žirgulis G, Bolander JE, Stang H. Influence of formwork surface on the orientation of steel fibres within self-compacting concrete and on the mechanical properties of cast structural elements. *Cem Concr Compos* 2014;50:60–72.
- [29] Xia J, Mackie K. Axisymmetric fiber orientation distribution of short straight fiber in fiber-reinforced concrete. *ACI Mater J* 2014;111(2):133–42.
- [30] Yoo DY, Kang ST, Yoon YS. Effect of fiber length and placement method on flexural behavior, tension-softening curve, and fiber distribution characteristics of UHPFRC. *Constr Build Mater* 2014;64:67–81.
- [31] Abrishambaf A, Barros JAO, Cunha VMCF. Tensile stress–crack width law for steel fibre reinforced self-compacting concrete obtained from indirect (splitting) tensile tests. *Cem Concr Compos* 2015;57:153–65.
- [32] Blanco A, Pujadas P, de la Fuente A, Cavalaro SHP, Aguado A. Assessment of the fibre orientation factor in SFRC slabs. *Compos – Part B: Eng* 2015;68:343–54.
- [33] Ferrara L. Tailoring the orientation of fibers in High Performance Fiber Reinforced Cementitious Composites: part 2 – correlation to mechanical properties and design implications. *J Mater Struct Integ* 2015;9(1/2/3):92–107.
- [34] Lameiras R, Barros JAO, Azenhab M. Influence of casting condition on the anisotropy of the fracture properties of Steel Fibre Reinforced Self-Compacting Concrete (SFRSCC). *Cem Concr Compos* 2015;59:60–76.
- [35] Yoo DY, Zi G, Kang ST, Yoon YS. Biaxial flexural behavior of ultra-high-performance fiber-reinforced concrete with different fiber lengths and placement methods. *Cem Concr Compos* 2015;63:51–66.
- [36] Bastien-Masse M, Denarié E, Brühwiler E. Effect of fiber orientation on the in-plane tensile response of UHPFRC reinforcement layers. *Cem Concr Compos* 2016;67:111–25.
- [37] Sarmiento EV, Geiker M, Kanstad T. Influence of fibre distribution and orientation on the flexural behaviour of beams cast from flowable hybrid polymer–steel FRC. *Constr Build Mater* 2016;109:166–76.
- [38] Žirgulis G, Švec O, Geiker M, Cwirzen A, Kanstad T. Variation in fibre volume and orientation in walls: experimental and numerical investigation. *Struct Concr* 2016. doi: <http://dx.doi.org/10.1002/suco.201500060>.

- [39] Žirgulis G, Švec O, Geiker M, Cwirzen A, Kanstad T. Influence of reinforcement bar layout on fibre orientation and distribution in slabs cast from fibre-reinforced self-compacting concrete (FRSCC). *Struct Concr* 2016. doi: <http://dx.doi.org/10.1002/suco.201500064>.
- [40] Guenet T. Modélisation du comportement des bétons fibrés à ultra-hautes performances par la micromécanique: effet de l'orientation des fibres à l'échelle de la structure, PhD thesis, Thèse en cotutelle Université Laval – Université Paris-Est, 31 mars 2016; 2016. p. 322.
- [41] Laranjeira F, Grünewald S, Walraven J, Blom C, Molins C, Aguado A. Characterization of the orientation profile of steel fiber reinforced concrete. *Mater Struct* 2011;44(6):1093–111.
- [42] Laranjeira F, Aguado A, Molins C, Grünewald S, Walraven J, Cavalaro SHP. Framework to predict the orientation of fibers in FRC: a novel philosophy. *Cem Concr Res* 2012;42:752–68.
- [43] Stroeven P, Shah SP. Use of radiography-image analysis for steel fiber reinforced concrete. In: Swamy RN, editor. *Testing and test methods of fiber cement composites*. Lancaster: Construction Press; 1978. p. 345–53.
- [44] Woo LY, Wansom S, Ozyurt N, Mu B, Shah SP, Mason TO. Characterizing fiber dispersion in cement composites using AC impedance spectrometry. *Cem Concr Compos* 2005;27:627–36.
- [45] Eik M, Lohmus K, Tigasson M, Listan M, Puttonen J, Herrmann H. DC-conductivity testing combined with photometry for measuring fiber orientations in SFRCs. *J Mater Sci* 2013;48(10):3745–59.
- [46] Ozyurt N, Woo LY, Mason TO, Shah SP. Monitoring fiber dispersion in fiber reinforced cementitious materials: comparison of AC impedance spectroscopy and image analysis. *ACI Mater J* 2006;103(5):340–7.
- [47] Ozyurt N, Mason TO, Shah SP. Non destructive monitoring of fiber orientation using AC-IS: an industrial scale application. *Cem Concr Res* 2006;36:1653–60.
- [48] Lataste JF, Behloul M, Breyse D. Characterisation of fibres distribution in a steel fibre reinforced concrete with electrical resistivity measurements. *Non Destruct Test Eng Int* 2008;41(8):638–47.
- [49] Barnett S, Lataste JF, Parry T, Millard SG, Soutsos MN. Assessment of fibre orientation in ultra high performance fiber reinforced concrete and its effect on flexural strength. *Mater Struct* 2010;43(7):1009–23.
- [50] Lataste JF, Barnett SJ, Parry T, Tsoutsos MN. Study of fiber distribution and orientations in UHPFRC by electrical resistivity and mechanical tests. *Eur J Environ Civil Eng* 2011;15(4):533–44.
- [51] Van Damme S, Franchois A, De Zutter D, Taerwe L. Nondestructive determination of the steel fiber content in concrete slabs with an open-ended coaxial probe. *IEEE Trans Geosci Remote Sens* 2009;47(11):2511–21.
- [52] Felicetti R, Ferrara L. The effect of steel fibre on concrete conductivity and its connection to on-site material assessment. In: Gettu R, editor. *Proceedings of Befib 2008, 7th international RILEM symposium on fiber reinforced concrete*, Chennai, India, 17–19 September 2008, RILEM Pubs.; 2008. p. 525–36.
- [53] Foudazi A, Mehdipour I, Donnel KM, Khayat KH. Evaluation of steel fiber distribution in cement based mortars using active microwave thermography. *Mater Struct* 2016. doi: <http://dx.doi.org/10.1617/s11527-016-0843-3>.
- [54] Liu J, Li C, Liu J, Cui G, Yang Z. Study on 3D spatial distribution of steel fibers in fiber reinforced cementitious composites through micro CT scans. *Constr Build Mater* 2013;48:656–61.
- [55] Suuronen JP, Kallonen A, Eik M, Puttonen J, Serinea R, Herrmann H. Analysis of short fibers orientation in steel fiber reinforced concrete (SFRC) by X-ray tomography. *J Mater Sci* 2013;48:1358–67.
- [56] Vicente MA, Gonzalez DC, Maynez J. Determination of dominant fibre orientations in fibre reinforced high strength concrete elements based on computed tomography scans. *Non Destruct Test Eval* 2014;29(2):164–82.
- [57] Zofka A, Paliukaiti M, Vaitkus A, Maliszewski D, Josku R, Bernier A. Laboratory study on the influence of casting on properties of ultra-high performance fiber reinforced concrete (UHPFRC) specimens. *J Civil Eng Manage* 2014;20(3):380–8.
- [58] Ponikiewski T, Katzer J, Bugdol M, Rudzki M. Steel fiber spacing in self-compacting concrete precast walls by X-ray computed tomography. *Mater Struct* 2015;48:3863–74.
- [59] Ponikiewski T, Golaszewski J, Rudzki M, Bugdol M. Determination of steel fibers distribution in self-compacting concrete beams using X-ray computed tomography. *Arch Civil Mech Eng* 2015;15(2):558–68.
- [60] Ponikiewski T, Katzer J, Bugdol M, Rudzki M. X-ray computed tomography harnessed to determine 3D spacing of steel fibers in self-compacting concrete (SCC) slabs. *Constr Build Mater* 2015;74:102–8.
- [61] Herrmann H, Pastorelli E, Kallonen A, Suuronen JP. Methods for fibre orientation analysis of X-ray tomography images of steel fibre reinforced concrete (SFRC). *J Mater Sci* 2016;51(8):3772–83.
- [62] Ponikiewski T, Katzer J. X-ray computed tomography of fiber reinforced self-compacting concrete as a tool of assessing its flexural behavior. *Mater Struct* 2016. doi: <http://dx.doi.org/10.1617/s11527-015-0638y>.
- [63] Bordelon AC, Roesler JR. Spatial distribution of synthetic fibers in concrete with X-ray computed tomography. *Cement Concr Compos* 2014;53:35–43.
- [64] Felekoglu B, Tomer-Felekoglu K, Guden E. A novel method for the determination of polymer micro-fiber distribution of cementitious composites exhibiting multiple cracking behavior under tensile loading. *Constr Build Mater* 2015;86 [p. 95–94].
- [65] Faifer M, Ottoboni R, Toscani S, Ferrara L. Non-destructive testing of steel fiber reinforced concrete using a magnetic approach. *IEEE Trans Instrum Meas* 2011;60(5):1709–17.
- [66] Torrents JM, Blanco A, Pujadas P, Aguado A, Juan-Garcia P, Sanchez-Moraguez MA. Inductive method for assessing the amount and orientation of steel fibers in concrete. *Mater Struct* 2012;45(10):1577–92.
- [67] Al-Mattarneh H. Electromagnetic quality control of steel fibre concrete. *Constr Build Mater* 2014;73:350–6.
- [68] Cavalaro SHP, Lopez R, Torrents JM, Aguado A. Improved assessment of fiber content and orientation with inductive method in SFRC. *Mater Struct* 2015;48(6):1859–73.
- [69] Cavalaro SHP, Lopez-Carreño R, Torrents JM, Aguado A, Juan-Garcia P. Assessment of fibre content and 3D profile in cylindrical SFRC specimens. *Mater Struct* 2016;49(1):577–95.
- [70] Faifer M, Ferrara L, Ottoboni R, Toscani S. Low frequency electrical and magnetic methods for non-destructive monitoring of fiber dispersion in fiber reinforced cementitious composites: an overview. *Sensors* 2013;13:1300–18.
- [71] Ferrara L, Faifer M, Toscani S. A magnetic method for non destructive monitoring of fiber dispersion and orientation in Steel Fiber Reinforced Cementitious Composites – part 1: method calibration. *Mater Struct* 2012;45(4):575–89.
- [72] Simulation of fresh concrete flow. State of the art report of the RILEM technical committee 222-SCF. In: Roussel N, Gram A, editors. *Springer*; 2014. p. 147.
- [73] Roussel N, Geiker M, Dufour F, Thrane LN, Szabo P. Computational modeling of concrete flow: general overview. *Cem Concr Res* 2007;37:1298–307.
- [74] Roussel N, Gram A, Cremonesi M, Ferrara L, Krenzer K, Mechtcherine V, et al. Numerical simulations of concrete flow: a benchmark comparison. *Cem Concr Res* 2016;69:265–71.
- [75] Mechtcherine V, Gram A, Krenzer K, Schwabe J-H, Shyshko S, Roussel N. Simulation of fresh concrete flow using DEM: theory and applications. *Mater Struct* 2014;47:615–30.
- [76] Shyshko S, Mechtcherine V. Developing a Discrete Element Model for simulating fresh concrete: experimental investigation and modelling of interactions between discrete aggregate particles with fine mortar between them. *Constr Build Mater* 2013;47:601–15.
- [77] Mechtcherine V, Shyshko S. Simulating the behaviour of fresh concrete with the distinct element method – deriving model parameters related to the yield stress. *Cem Concr Compos* 2015;55:81–90.
- [78] Ferrara L, Shyshko S, Mechtcherine V. Predicting the flow-induced dispersion and orientation of steel fibers in SCC by DEM. In: Barros J, et al., editor. *Proceedings BEFIB 2012, Guimaraes, Portugal, September 20–22, 2012, RILEM Pubs.*; 2012. p. 12.
- [79] Jeffery GB. The motion of ellipsoidal particles immersed in a viscous fluid. *Proc Roy Soc Lond A* 1923;102:161–79.
- [80] Folgar F, Tucker III CF. Orientation behavior of fibers in concentrated suspensions. *J Reinf Plast Compos* 1984;3:98–119.
- [81] Advani SG, Tucker III CF. The use of tensors to describe and predict fiber orientation in short fiber composites. *J Rheol* 1987;31(8):751–84.
- [82] Dupont D, Vandewalle L. Distribution of steel fibres in rectangular sections. *Cem Concr Compos* 2005;27:391–8.
- [83] Martinie L, Lataste JF, Roussel N. Fiber orientation during casting of UHPFRC: electrical resistivity measurements, image analysis and numerical simulations. *Mater Struct* 2015;48(4):947–57.
- [84] Ferrara L, Tregger N, Shah SP. Flow-induced fiber orientation in SCSFRC: monitoring and prediction. In: Khayat KH, Feys D, editors. *Proceedings SCC2010, Montreal, Canada: Springer*; 2010. p. 417–28.
- [85] Ferrara L, Cremonesi M. Effects of casting process on toughness properties of fiber reinforced-self compacting concrete as from EN 14651. In: Roussel N, Bessaies-Bey H, editors. *Proceedings 7th RILEM international conference on self compacting concrete and 1st RILEM international conference on rheology and processing of construction materials, Paris, France, 1–3 September; 2013, CD-Rom*.
- [86] Orbe A, Losada R, Roji E, Cuadrado J. The prediction of bending strengths in SFRC using Computational Fluid Dynamics (CFD). *Constr Build Mater* 2014;66:587–96.
- [87] Švec O. Flow modelling of steel fibre reinforced self-compacting concrete. Technical University of Denmark; 2013.
- [88] Cremonesi M, Frangi A, Perego U. A Lagrangian finite element approach for the analysis of fluid-structure interaction problems. *Int J Numer Meth Eng* 2010;84(10):610–30.
- [89] Cremonesi M, Ferrara L, Frangi A, Perego U. Simulation of the flow of fresh cementitious suspensions by a Lagrangian Finite Element approach. *J Non-Newton Fluid Mech* 2010;165:1555–63.
- [90] Baril M. Effet de défauts de coulage sur la micro-fissuration des dalles minces en béton fibre à ultra-hautes performances par stéréovision et corrélation d'images digitales. Master Thesis, Université Laval, Avril; 2016.
- [91] Ferrara L, Cremonesi M, Tregger N, Frangi A, Shah SP. On the identification of rheological properties of cement suspensions: rheometry, computational fluid dynamics modeling and field test measurements. *Cem Concr Res* 2012;42:1134–46.
- [92] Ferrara L, Haist M. Rheological characterization of high performance fiber reinforced cementitious composites. In: Barros J, et al. editor. *Proceedings BEFIB 2012, Guimaraes, Portugal, September 20–22, 2012, RILEM Pubs.*; 2012. p. 12.
- [93] Baril MA, Sorelli L, Rethore J, Baby F, Toutlemonde F, Ferrara L, Bernardi S, Fafard M. Effect of Casting Flow Defects on the Crack Propagation in UHPFRC Thin Slabs by Means of Stereovision Digital Image Correlation. *Constr Build Mater* 2016;129:182–92.